European Journal of Pharmaceutical Sciences 203 (2024) 106922

Contents lists available at ScienceDirect

European Journal of Pharmaceutical Sciences

journal homepage: www.elsevier.com/locate/ejps

Characterising and preventing the gut microbiota's inactivation of trifluridine, a colorectal cancer drug

Laura E. McCoubrey [a,1], Chenghao Shen [a], Sydney Mwasambu [b], Alessia Favaron [a], Nannapat Sangfuang [a], Stavrina Thomaidou [a], Mine Orlu [a], Daniel Globisch [b], Abdul W. Basit [a,*]

[a] UCL School of Pharmacy, 29-39 Brunswick Square, London, WC1N 1AX, United Kingdom
[b] Department of Chemistry - BMC, Science for Life Laboratory, Uppsala University, 75124 Uppsala, Sweden

ARTICLE INFO

Keywords:
Biotransformation
Pharmacomicrobiomics
Drug-microbiome interactions
Colonic drug delivery
Formulation design
Personalised medicine
Gut microbiota

ABSTRACT

The gut microbiome can metabolise hundreds of drugs, potentially affecting their bioavailability and pharmacological effect. As most gut bacteria reside in the colon, drugs that reach the colon in significant proportions may be most impacted by microbiome metabolism. In this study the anti-colorectal cancer drug trifluridine was used as a model drug for characterising metabolism by the colonic microbiota, identifying correlations between bacterial species and individuals' rates of microbiome drug inactivation, and developing strategies to prevent drug inactivation following targeted colonic delivery. High performance liquid chromatography and ultra-high performance liquid chromatography coupled with high resolution tandem mass spectrometry demonstrated trifluridine's variable and multi-route metabolism by the faecal microbiota sourced from six healthy humans. Here, four drug metabolites were linked to the microbiome for the first time. Metagenomic sequencing of the human microbiota samples revealed their composition, which facilitated prediction of individual donors' microbial trifluridine inactivation. Notably, the abundance of *Clostridium perfringens* strongly correlated with the extent of trifluridine inactivation by microbiota samples after 2 hours ($R^2 = 0.8966$). Finally, several strategies were trialled for the prevention of microbial trifluridine metabolism. It was shown that uridine, a safe and well-tolerated molecule, significantly reduced the microbiota's metabolism of trifluridine by acting as a competitive enzyme inhibitor. Further, uridine was found to provide prebiotic effects. The findings in this study greatly expand knowledge on trifluridine's interactions with the gut microbiome and provide valuable insights for investigating the microbiome metabolism of other drugs. The results demonstrate how protection strategies could enhance the colonic stability of microbiome-sensitive drugs.

1. Introduction

Hundreds of drugs are now known to be susceptible to gut microbiome metabolism (Javdan et al., 2020; Zimmermann et al., 2019). In a number of cases, microbiome metabolism has been demonstrated to alter the pharmacokinetics and/or pharmacodynamics of drugs to a clinically significant extent (Lee et al., 2015; Mehta et al., 2023; Spanogiannopoulos et al., 2022; Tian et al., 2023; van Kessel et al., 2019). Despite this, investigation of new drugs' interactions with the gut microbiota is rare and represents an under-explored area of pharmaceutical research. This may lead to the selection of drug candidates with unexplained pharmacokinetic variability, arising from inter-individual differences in gut microbiome composition. In addition, drugs may suffer from low bioavailability, especially in the distal gastrointestinal (GI) tract where microbial density is highest (Martinez-Guryn et al., 2019). Poor bioavailability in the distal GI tract could complicate the development of extended and targeted release formulations, thus presenting challenges for once daily dosing or local treatment of GI diseases (Verstockt et al., 2022). As such, characterising the microbiome stability of drugs, especially those expected to reach the distal GI tract in significant proportions, could increase their chances of clinical success.

Gut microbiome composition varies greatly between individuals, potentially leading to differences in microbial drug metabolism (Javdan et al., 2020). For several drugs the abundance of certain bacterial strains or enzymes in patients' faeces has been correlated with therapeutic efficacy (Lee et al., 2015; Mehta et al., 2023; Tian et al., 2023; van Kessel

* Corresponding author.
E-mail address: a.basit@ucl.ac.uk (A.W. Basit).
[1] Now at GlaxoSmithKline R&D, Ware, United Kingdom

https://doi.org/10.1016/j.ejps.2024.106922
Received 17 June 2024; Received in revised form 1 October 2024; Accepted 2 October 2024
Available online 3 October 2024

et al., 2019). Therefore, once susceptibility to drug microbiome metabolism has been confirmed, the ability to predict how it will vary across the target patient population would provide sophisticated insight into causes of pharmacokinetic variability. Further, as medicine moves towards a more personalised framework, prediction of individual patients' microbial drug metabolism rate could aid with the selection of personalised doses.

Microbiome drug metabolism can reduce the bioavailability of drugs and provide a source of pharmacokinetic variability. As such, strategies to protect drugs from degradation by the gut microbiota could be highly useful. At present very little research has been dedicated to the development of preventative strategies. One example was published by Haiser et al, wherein the bacterial metabolism of digoxin was shown to be inhibited by arginine (Haiser et al., 2013). Here, microbial metabolism of digoxin was reduced when mice were fed a high-protein diet due to arginine's suppression of the metabolising bacterial gene. This work provided evidence that microbiome drug metabolism could be prevented locally and impermanently in the gut. Despite this, no strategies for the microbial protection of drugs have been tested clinically.

In this study trifluridine was selected as a model drug for the characterisation and prevention of microbiome metabolism. Trifluridine is marketed as the film-coated tablet Lonsurf®, which is a third-line option for the treatment of metastatic colorectal cancer (Servier Laboratories Limited, 2020). Trifluridine is the antineoplastic agent within Lonsurf®, acting as a thymidine-based nucleoside analogue that incorporates into cancer cell DNA to prevent proliferation. Tipiracil is also an essential component of Lonsurf® as it reduces intracellular inactivation of trifluridine by thymidine phosphorylases and potentiates antitumour efficacy (Kang et al., 2019). As Lonsurf® is formulated as a standard film-coated tablet, trifluridine is released in the upper GI tract (Center for Drug Evaluation and Research, 2015; Servier Laboratories Limited, 2020). The efficacy of trifluridine treatment for colorectal cancer could potentially be improved by site-specific delivery to the colon, as drug concentration would be optimised at the site of colorectal tumours (Yadav et al., 2022). Colonic drug delivery can be reliably achieved with advanced formulation systems (Allegretti et al., 2019; Peiris et al., 2022; Varum et al., 2020a; Varum et al., 2020b). However, work by Javdan et al. has indicated that trifluridine is significantly transformed by the intestinal microbiota via deglycosylation to an inactive metabolite, trifluorothymine (Fig. 1) (Javdan et al., 2020). This microbiome metabolism would likely impair the colonic stability of trifluridine and may also contribute towards its low bioavailability when administered as a standard release formulation (due to possible inactivation by the small intestinal microbiota). As such, better understanding and management of trifluridine's microbial inactivation could pave the way for a more efficacious colorectal cancer treatment.

This study aimed to characterise and prevent microbiome-mediated trifluridine inactivation. Variability in drug metabolism between different humans' microbiomes was first explored using high performance liquid chromatography (HPLC) and ultra-high performance liquid chromatography coupled with high resolution tandem mass spectrometry (LC-MS). This characterisation revealed the formation of five drug metabolites; four of which were detected in human microbiome samples for the first time. Linear regression was then used to identify correlations between samples' composition and the extent that different individuals' microbiota would metabolise trifluridine within 2 hours. Various methods of preventing trifluridine inactivation were subsequently trialled and the effects of these interventions on the microbiota were assessed. This workflow represents a strategic investigation and management plan for microbiome drug metabolism that could be applied during the development of other microbiome-sensitive drugs.

2. Materials and methods

2.1. Materials

Trifluridine was purchased from Generon (Slough, UK). Bryant and Burkey medium (BBM), ¼ Ringer's tablets, and triethylamine were purchased from Merck Life Science (Gillingham, UK). Uridine, agar powder, and HPLC-grade acetonitrile were purchased from Thermo Fisher Scientific (Loughborough, UK). Phosphoric acid was purchased from Honeywell Fluka (Bracknell, UK). Trifluorothymine and tipiracil hydrochloride were purchased from Insight Biotechnology (Wembley, UK). Clindamycin was purchased from Cambridge Bioscience (Cambridge, UK). Bidistilled glycerol was purchased from VWR International (Pennsylvania, USA). All other reagents were of HPLC grade.

2.2. Methods

2.2.1. Collection and culture of human faecal microbiota

Faecal samples were sourced from six healthy volunteers (n = 3 for males; n = 3 females) who were aged 27 - 35, had not taken oral antibiotics for at least 12 months, and had a variety of ethnicities. The donors had a variety of diets, including two vegetarians (n = 1 male and female). Ethical approval to collect human faeces was obtained by Intract Pharma Ltd. from the UCL Biobank Ethical Review Committee at Royal Free London NHS Foundation Trust (reference no. NC2017.010).

Fig. 2 demonstrates the protocol used to obtain and culture human faecal microbiota. Each donor deposited a fresh faecal sample into a plastic receptacle and immediately added an AnaeroGen sachet (Thermo Fisher Scientific, Loughborough, UK) into the receptacle before closing the lid to generate an anaerobic atmosphere within. Maintaining an anaerobic environment during the storage and processing of the samples was important to protect the viability of the microbiota. Faecal samples were stored overnight at - 20°C and subsequently moved into an anaerobic chamber (Electrotek 500TG workstation, Electrotek, West Yorkshire, UK) set at a temperature of 37°C and 70 % relative humidity, to support optimal culturing, the next morning. 25 % w/w faecal slurries were then produced by combining and homogenising faecal samples

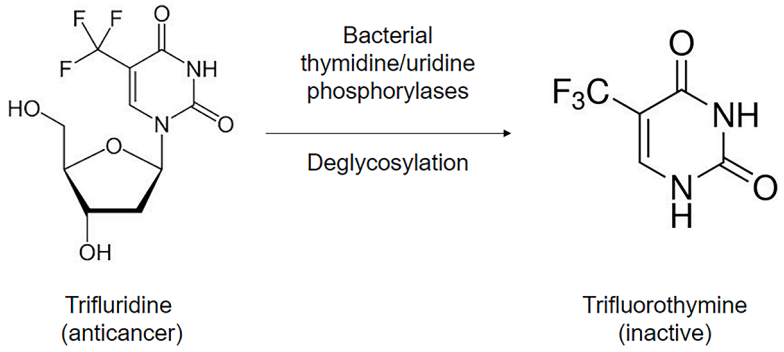

Fig. 1. The microbial transformation of trifluridine to its inactive metabolite, trifluorothymine, as characterised by reference (Javdan et al., 2020).

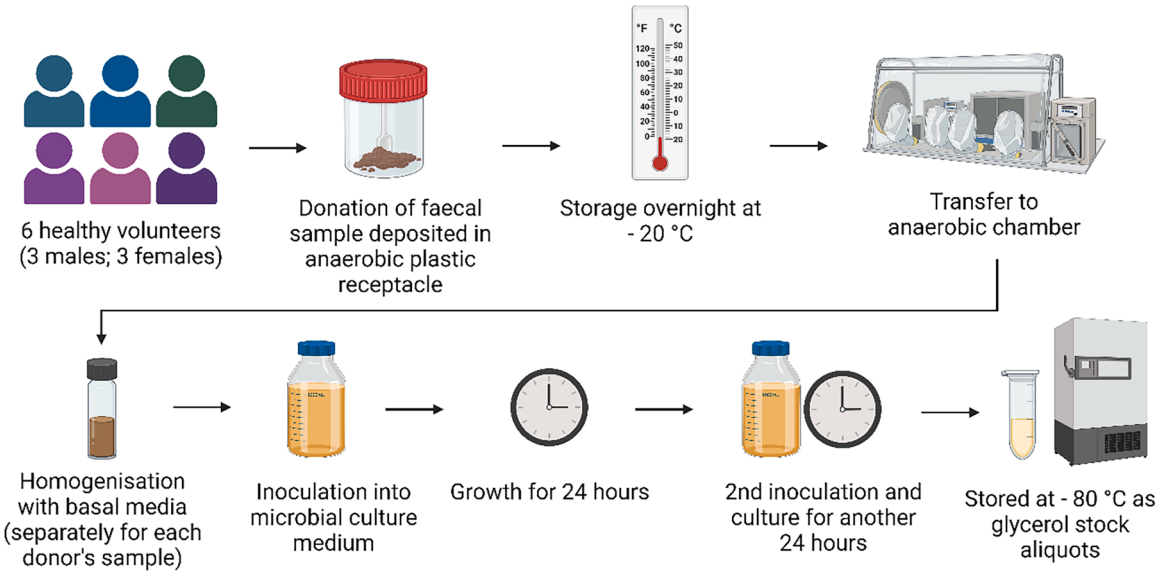

Fig. 2. The protocol for acquiring and processing aliquots of human faecal microbiota. This process was conducted for each donor thereby generating microbial samples from each individual.

with basal media at a ratio of 1:3. The basal media was added to produce liquid slurries from the faecal samples whilst preserving microbial viability. Basal media composition was the same as that used in a previous study (Yadav et al., 2021). Next, 0.50 mL faecal slurry was inoculated into 100 mL sterilised BBM and incubated for 24 hours under anaerobic conditions to allow the faecal microbiota to establish. Cultures were agitated on an orbital shaker (IKA VXR Basic Vibrax® Orbital Shaker (IKA-Werke, Staufen, Germany) at 100 rpm. 1.0 mL of the resulting culture was then inoculated into a second 100 mL sterile BBM and incubated for a further 24 hours under anaerobic conditions. This second culture step was performed to obtain stable and abundant samples. The final culture was subsequently mixed with 30 % glycerol in ¼ Ringer's solution to obtain a 15 % v/v glycerol stock suspension and frozen in aliquots at - 80°C for each donor. Here, ¼ Ringer's solution and glycerol were added to support microbial viability during freezing and storage. Aliquots were only used once to avoid multiple freeze-thaw cycles and preserve microbial viability (Karatza et al., 2016).

Faecal samples were processed in this way to obtain many aliquots of faecal microbiota originating from each individual. An advantage of this protocol includes the ability to conduct multiple experiments on microbial aliquots sourced from a single faecal sample, hence limiting variability and facilitating inclusion of technical replicates. Biological variability was captured by testing the microbiota sourced from several different individuals. Furthermore, the unwanted elements of faecal samples (such as undigested polysaccharides) were processed out of samples via the two culture steps. BBM was chosen as a culture medium as it has been previously shown to preserve the richness of faecal cultures whilst preventing overexpansion of certain species (Javdan et al., 2020; Tao et al., 2023). However, it is certain that the composition of the final microbial aliquots would be, even slightly, different to that of the original faecal samples. This is a limitation of the protocol, although it was accepted due to the aforementioned advantages and the fact that similar processing has been performed in high-impact publications (Javdan et al., 2020). As such, the depletion of drugs by these faecal cultures may not directly correlate with the rate of drug metabolism *in vivo*. However, the samples were deemed to be appropriate for assessing the likelihood of depletion occurring *in vivo* (a prediction for metabolism *vs*. no metabolism) and could be validated for this if depletion data in humans were to become available.

Immediately prior to use, aliquots were thawed within an anaerobic chamber (A25 Sleeved Anaerobic Workstation, Don Whitley Scientific, Bingley, UK; containing 5 % CO_2, 5 % H_2, 90 % nitrogen) set at 37°C and vortexed for 15 seconds. The microbial density of each donor's microbiota samples was calculated by serially diluting one thawed aliquot per donor (from 10^2 - 10^{11} dilution factor) in phosphate buffered saline and plating on solid media composed of BBM and 1.20 % agar powder. Plates were incubated anaerobically for 72 hours at 37°C then colonies were visually counted, allowing the calculation of the CFU present in each millilitre of sample.

2.2.2. *Measuring microbial metabolism of trifluridine*

A microbiota sample from each donor was thawed, vortexed, and 0.75 mL was inoculated into 75 mL autoclaved BBM inside an anaerobic chamber (A25 Sleeved Anaerobic Workstation, Don Whitley Scientific, Bingley, UK; containing 5 % CO_2, 5 % H_2, 90 % nitrogen) maintained at 37°C. The microbiota was cultured overnight; cultures were agitated on an orbital shaker (IKA VXR Basic Vibrax® Orbital Shaker (IKA-Werke, Staufen, Germany) at 100 rpm.

In the morning the OD of each donor's culture was measured using a cell density meter set at a 600 nm wavelength (CO 8000 Biowave, VWR International, Pennsylvania, USA). 5.0 mL of each culture was then transferred to autoclaved glass vials (n = 3 each donor culture). To each 5.0 mL culture, 5.0 mL of 400 μg/mL trifluridine in BBM solution was added and mixed, creating a 200 μg/mL (675 μM) starting incubation concentration. This concentration reflects the concentration of the maximum single dose of trifluridine (80 mg) dissolved in the average fluid volume in healthy volunteers' ascending and transverse colons (401 mL) (Pritchard et al., 2014). Trifluridine was weighed and dissolved in the BBM aseptically using sterile vials and spatulas to avoid contamination of incubations with external microorganisms. Incubation vials were agitated on an orbital shaker (IKA VXR Basic Vibrax® Orbital Shaker (IKA-Werke, Staufen, Germany) at 100 rpm.

Trifluridine degradation was measured by sampling 600 μL incubation fluid at 0, 1, 2, 4, 6, and 24 hours and adding 600 μL acetonitrile to prevent further microbial activity. Incubations were conducted for 24 hours, as this is around the average colonic transit time of humans (Awad et al., 2022; McConnell et al., 2008). Timepoint samples were centrifuged at 10,000 g for 10 min at 4°C and the supernatant passed through sterile 0.22 μm PES filters (Millex™, Merck Life Science, Gillingham, UK) into amber glass HPLC vials (for HPLC analysis) or Eppendorf tubes (for LC-MS analysis). Samples were stored at 2 – 8°C before HPLC analysis, which was conducted within 5 days of the

incubation. Samples were frozen at – 80°C prior to LC-MS analysis. HPLC and MS allowed the quantification of trifluridine, trifluorothymine, and other metabolites' concentrations at each timepoint. Controls in this study included incubation of 200 μg/mL trifluridine in clean growth medium (microbiota-free) and incubation of the microbiota in the absence of trifluridine (microbiota-only). The microbiota-free control assessed trifluridine stability in the absence of the microbiota; the microbiota-only control was used to ensure that microbial metabolites produced during incubation did not interfere with HPLC/LC-MS analysis. Sterile drug-free BBM (clean broth control) was also analysed via HPLC for the same reason.

2.2.3. HPLC detection of trifluridine and its metabolites

2.2.3.1. High performance liquid chromatography. Table 1 shows the isocratic HPLC method used to detect trifluridine and its inactive metabolite trifluorothymine, adapted from a method in the literature (Eluru and Babu, 2020). Calibration curves were constructed by dissolving trifluridine and trifluorothymine together in BBM and acetonitrile (1:1 BBM:ACN ratio) at ranges of 10 – 120 μg/mL trifluridine and 6.0 – 72 μg/mL trifluorothymine, with six concentration points for both compounds. Calibration curves were generated during initial HPLC method assessment and at the beginning and end (n = 2 calibration runs) of each HPLC run containing experimental samples. The R^2 for the trifluridine calibration curve was 0.999 and 0.998 for trifluorothymine (Figs. S1 and S2). Calibration standards were prepared by centrifuging solutions at 10,000 g at 4°C for 10 min and then passing solutions through sterile 0.22 μm PES filters (Millex™, Merck Life Science, Gillingham, UK) into amber glass HPLC vials. Quality control (QC) samples with known trifluridine and trifluorothymine concentrations (n = 3: low, medium, and high concentrations within the calibration ranges) were run with each calibration curve and the accuracy of the HPLC method was assessed by calculating the samples' relative standard deviations (RSD) from the linear calibration curve. The lower limits of quantification (LOQ) were set using a maximal signal-to-noise ratio of 2:1 compared to microbiota-only controls, as per ICH guidelines (International Council for Harmonisation of Technical Requirements for Pharmaceuticals for Human Use, 1995).

2.2.3.2. Ultra-high performance liquid chromatography–mass spectrometry

2.2.3.2.1. Sample preparation. 100 μL of each incubation timepoint sample (See Section 2.2.2) was thawed and aliquoted into a new Eppendorf tube. 400 μL of LC-MS grade methanol was added to each sample. The Eppendorf tubes were then vortexed for a few seconds and stored at - 20 °C for one hour to precipitate the proteins. The sample was then centrifuged for five minutes at 14,500 rpm and 4 °C, and the supernatant was transferred into another labelled Eppendorf tube. The solvent was evaporated in a SpeedVac for 1 h 30 minutes in V-AL mode, then for 1 h in V-AQ. To reconstitute the sample resulting pellets were dissolved in into Milli-Q H_2O/ACN (95%/5%, 50 μL) and then transferred into amber LC-MS vials for LC-MS^2 analysis.

2.2.3.2.2. Mass spectrometric analysis. The UHPLC-MS/MS analysis was performed in a Maxis II ETD Q-TOF mass spectrometer (Bruker Daltonics, Germany) using an electrospray ionization (ESI) source with an Elute UHPLC (Bruker Daltonics, Germany) system. Milli-Q water with 0.1% formic acid was used as mobile phase A and LC-MS grade methanol with 0.1% formic acid was used as mobile phase B. The column temperature was maintained at 40°C, and the autosampler temperature at 4°C. The flow rate was set to 0.2 mL/min. The gradient used was as follows: 0–2 min, 0% B; 2–15 min, 0–100% B; 15–16 min, 100% B; 16–17 min, 100–0% B; 17–23 min, 0% B. The system was controlled using the Compass HyStar software package from Bruker (Bruker Daltonics, Germany). High-resolution mass spectra were acquired in positive mode at a mass range of m/z 50–1200. Data acquisition was performed in AutoMSMS mode (data dependent acquisition, DDA) with ramped collision energy from 20 eV to 50 eV. A solution of sodium formate (10 mM in a mixture of 2-propanol/water (1/1, v/v)) was used for internal calibration at the beginning of each run, in a segment between 0.10 and 0.31 min.

Identification of trifluridine metabolites was conducted in a strategic manner according to literature data. Human metabolism of trifluridine has been reported to generate metabolites 2 (5-carboxy-2'-deoxy-uridine) and 4 (trifluorothymine), as shown in Fig. 3 (Pavan-Langston and Nelson, 1979; Voutsadakis, 2021). Additionally, metabolites 2, 3 (uracil-5-carboxylic acid), 4, 5 (5,6-dihydroxy-5-(trifluoromethyl)dihydropyrimidine-2,4(1H,3H)-dione) and 6 (3,3,3-trifluoro-2-(ureidomethyl) propanoic acid) have been characterised following intraperitoneal administration to mice via ^{19}F NMR spectroscopy (Fig. 3) (Tandon et al., 1992).

For MS/MS fragmentation analysis of metabolites 5 and 6, scheduled precursor list (SPL) mode was utilised with the first window at 12 min for 5 and 2 min for 6. All 5 identified metabolites (Fig. 3, Table S1) were validated using MS^2 spectra from fragmentation analysis as exemplified in Fig. S3. This validation represents structure elucidation at confidence level 2 (Schymanski et al., 2014; Vallianatou et al., 2021) The MS-data pre-processing using the XCMS platform in R identified 16,656 features which was reduced to 12,632 features using the following criteria; retention time deviation was not more than 60 seconds in either direction, intensity level was higher than a 20,000-ion count, and there was a 10 ppm mass accuracy. During analysis of the metabolites, the peak area at 0 h was subtracted from the 24 h timepoint to remove the mass spectrometric background noise.

Table 1
HPLC method used to detect trifluridine and trifluorothymine.

Parameter	Specification
HPLC machine	Agilent 1260 Infinity II (California, US)
Mobile phase composition	A: 0.1 % triethylamine in HPLC grade water, pH adjusted to 2.50 with phosphoric acid B: acetonitrile
Mobile phase ratio	A: 65 % B: 35 %
Flow rate	1.0 mL/min
Injection volume	10 μL
Detection wavelength	261 nm
Column	Reversed phase Roc C18 (150 × 4.6 mm), 5 μm particle size, 100 Å pore size (Restek, Pennsylvania, US)
Column temperature	Uncontrolled
Run time (min)	2.80
Trifluridine retention time (min)	1.70
Trifluorothymine retention time (min)	1.92

2.2.4. Metagenomic sequencing of the faecal microbiota

2.2.4.1. DNA extraction and sequencing. Metagenomic sequencing of the faecal microbiota samples was performed by Eurofins (Luxembourg), using their INVIEW metagenome package. The frozen microbial aliquots (n = 1 per donor) were thawed and inactivated with methanol (ratio 1:1), refrozen and shipped to Eurofins on dry ice. Upon arrival DNA was extracted and standard DNA library preparation for next generation Illumina sequencing was performed. This involved converting the DNA to fragments, ligating adapters to the end of DNA fragments, and finally amplifying the fragments using Illumina's proprietary flow cell (Illumina Inc., San Diego, US) (Illumina, 2010). Paired-end sequencing was then completed whereby fluorescently tagged nucleotides were assembled to complement the amplified DNA fragments on the flow cell. Illumina technology uses a proprietary process to read these assembling nucleotides called Sequencing-by-Synthesis, which relies on the characteristic fluorescent signal emitted as each nucleotide is added to the complementary DNA strand (Buermans and den Dunnen, 2014). Reading the wavelength and

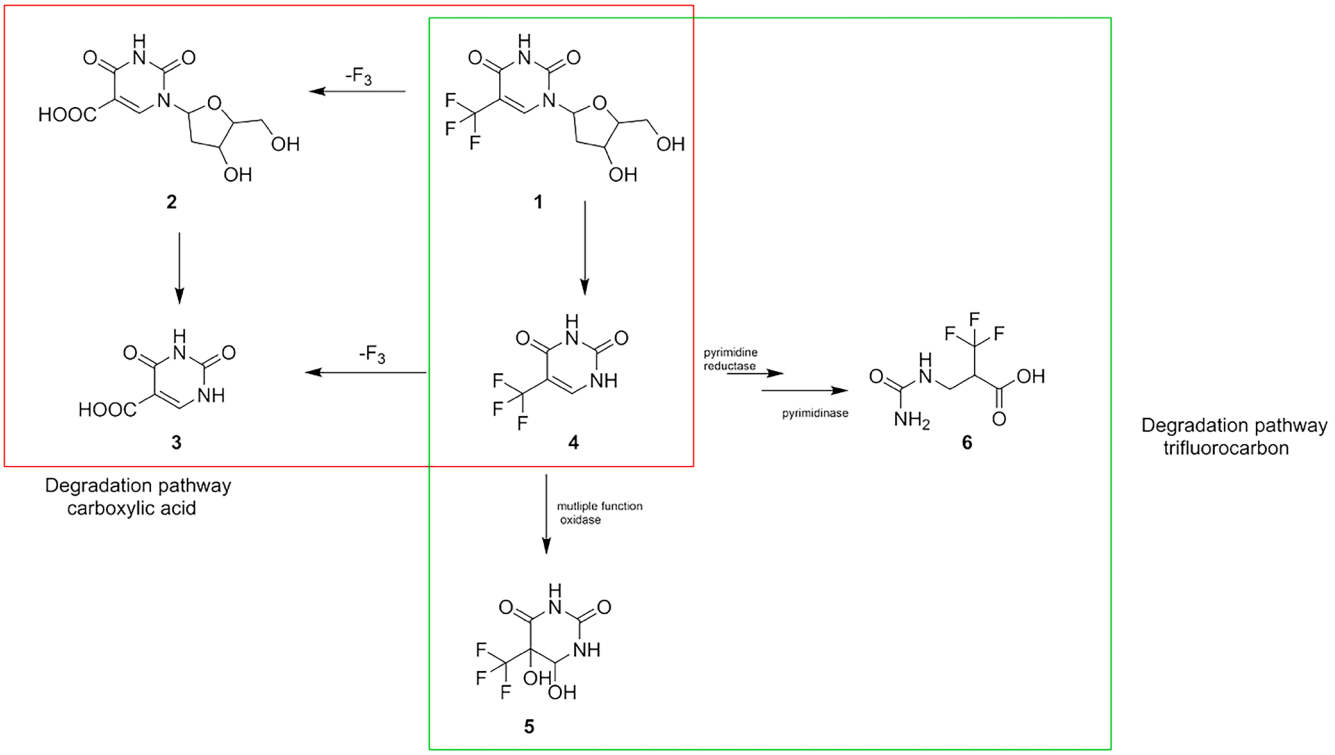

Fig. 3. Two major biotransformation pathways of trifluridine (compound 1). Metabolites 2 – 6 were sought in the microbiome incubation samples.

intensity of the fluorescent emissions allows interpretation of millions of DNA fragments' sequences simultaneously. Both directions of the DNA fragments were read in this manner.

2.2.4.2. Cleaning of sequence data. Raw sequencing data was cleaned by trimming adapter sequences and pruning poor quality bases from each read, using the fastp software (Chen et al., 2018). Poor quality bases were removed from reads using a sliding window approach which analysed regions' Phred Quality score (base call accuracy) that was generated during sequencing. Where the average Phred Quality within a region was < 20, meaning that average base call accuracy was < 90 %, then the bases were removed from further analysis. In addition, short reads of < 30 base pairs were also removed to retain only quality sequences that could be accurately mapped to reference genomes.

2.2.4.3. Analysis of sequence data. After sequence cleaning, the percentage of reads determined as high quality (Q30 Phred Quality, 99.9 % base call accuracy) was 98.82 - 99.12 % for all samples. Reads relating to human (host) DNA were identified and removed using the Kraken program (Wood and Salzberg, 2014). Briefly, the program identified reads of human origin by breaking reads into overlapping k-mers which could be individually mapped to reference genomes. The percentage of reads found to relate to human DNA was 0.06 - 0.08 % for all donor samples except Female 1, which had a higher percentage of 4.72 %. Assignment of the retained reads to microbial species (including bacteria, archaea, eukaryotes, and viruses) was completed using the MetaPhlAn (Metagenomic Phylogenetic Analysis) tool (Truong et al., 2015). The MetaPhlAn tool classified DNA by searching for marker genes within samples from around 17,000 reference genomes. Remaining unclassified reads were subsequently classified using Kraken and KrakenUniq, which broke reads into overlapping k-mers that could be mapped to taxa within a reference database (Breitwieser et al., 2018; Wood and Salzberg, 2014).

For all samples, the percentage of reads that were assigned to bacterial species (compared to other microorganism kingdoms) was ≥ 98.62 %. To enable comparison of species abundance between samples, the read counts of individual microbial species were normalised using the rarefy function within the vegan bioconductor package in R (Jari Oksanen et al., 2013). The functional profiles of microbial genes were then assigned using the HUMAnN (the HMP Unified Metabolic Analysis Network) tool (Beghini et al., 2021). Here, functions were assigned to species' genes using the MetaPhlAn and UniRef protein databases and gene family abundances (in counts per million (CPM) genes) were calculated (Suzek et al., 2015). In this manner, the abundances of thymidine and uridine phosphorylase genes (known to metabolise trifluridine) within samples and specific species could be measured.

Finally, the presence of antimicrobial resistance genes within samples was analysed using the Graphing Resistance Out Of meTagenomes (GROOT) software which located antimicrobial resistance genes via an indexing and similarity-search scheme that utilised a reference database of > 6000 antimicrobial resistance genes (Rowe and Winn, 2018).

2.2.5. Identifying correlations between microbial composition and trifluridine metabolism

Linear regression was employed to identify correlations between donors' samples and their metabolism of trifluridine. Regression was applied to the features associated with the microbiota samples (Table 2) and their average extent of trifluridine inactivation after 2 hours, as measured by HPLC. The coefficient of determination (R^2) was used to quantify correlations. A t-test was used to investigate whether the feature with the strongest correlation had significantly different values between the 'slow' trifluridine metabolising samples (< 50 % metabolised at 2 hours, $n = 3$) and the 'fast' metabolising samples (> 86 % metabolised at 2 hours, $n = 3$).

The features used for linear regression are presented in Table 2; they were chosen to capture the samples' microbial density, their genetic trifluridine-metabolising potential, and their taxonomy at the genus and species levels. Each sample contained thousands of bacterial species, viruses, fungi, and archaea, however the most abundant genera ($n = 13$) and species ($n = 22$) were selected as features to limit the feature set size and provide broad comparisons of samples' taxonomies. Samples' genetic trifluridine-metabolising potential was inferred from their total

Table 2
The features used to assess individual donors' microbial metabolism of trifluridine. The microbial density of the stock culture was measure via plating, as outlined in Section 2.2.1. The optical density (OD) of the cultures was measured after 24 hours growth, as outlined in Section 2.2.7. The abundance of thymidine/uridine phosphorylase genes was extracted from the functional profiling of samples' metagenomes using gene ontology mapping (Ashburner et al., 2000). The abundance of the top 13 most common genera and 22 species within samples was obtained from taxonomic profiling of metagenomic data via MetaPhlAn (Truong et al., 2015). CPM: counts per million genes.

Microbial density of samples	Relative abundance of genes known to encode for trifluridine-metabolising enzymes (CPM)	Relative abundance of most prevalent genera (%)	Relative abundance of most prevalent species (%)	
Microbial density in stock culture (CFU/mL)	Thymidine phosphorylase	*Bacteroides*	*Bacteroides fragilis*	*Ruminococcus torques*
Optical density after 24 hours incubation	Uridine phosphorylase	*Enterococcus*	*Bacteroides thetaiotaomicron*	*Dorea formicigenerans*
		Lactobacillus	*Bacteroides uniformis*	*Dorea longicatena*
		Clostridium	*Bacteroides vulgatus*	*Fusicatenibacter saccharivorans*
		Eubacterium	*Enterococcus durans*	*Faecalibacterium prausnitzii*
		Blautia	*Enterococcus faecalis*	*Flavonifractor plautii*
		Dorea	*Enterococcus faecium*	*Ruminococcus faecis*
		Fusicatenibacter	*Enterococcus hirae*	*Peptoniphilus harei*
		Faecalibacterium	*Lactobacillus delbrueckii*	*Sutterella wadsworthensis*
		Flavonifractor	*Clostridium baratii*	
		Ruminococcus	*Clostridium perfringens*	
		Peptoniphilus	*Eubacterium ramulus*	
		Sutterella	*Blautia obeum*	

abundance of thymidine and uridine phosphorylase genes; the two genes known to metabolise trifluridine *ex vivo* (Javdan et al., 2020). The feature values for each donor are presented in Table S2.

2.2.6. Preventing microbial trifluridine metabolism

Three test compounds were selected for their hypothesised ability to prevent microbial trifluridine metabolism: clindamycin, tipiracil hydrochloride, and uridine. To study their effect on trifluridine metabolism, the test compounds were separately added into incubation vials containing 10 mL human faecal microbiota culture (Female Donor 2) and 200 μg/mL trifluridine, as described in Section 2.2.2. The microbiota from Female Donor 2 was used for incubations as it resulted in a rapid rate of trifluridine metabolism during the experiments examining inter-individual variability.

Clindamycin was chosen as a model antibiotic to characterise trifluridine metabolism when microbial growth was prevented, as it has significant activity against the gut microbiota (Shaw et al., 2019). Clindamycin was incubated at 1.0 mg/mL (n = 3) to ensure antibacterial action and mimic its high concentrations recorded in patient faeces (Steinbakk et al., 1992). Tipiracil hydrochloride was incubated at a concentration of 81.83 μg/mL (n = 3), to reflect the ratio of trifluridine and tipiracil hydrochloride found in the marketed formulation, Lonsurf® (Servier Laboratories Limited, 2020). Uridine was incubated at three concentrations: low (5.0 mg/mL), medium (15 mg/mL), and high (35 mg/mL) (n = 3 each concentration) to examine whether concentration-dependent saturation of one of trifluridine's inactivating enzymes (uridine phosphorylase) was possible. As in Section 2.2.2, timepoint samples were taken at 0, 1, 2, 4, 6, and 24 hours and their trifluridine and trifluorothymine concentrations were assessed using HPLC.

2.2.7. The effect of trifluridine, tipiracil, clindamycin and uridine on microbial growth

The OD (600 nm) of the microbiota-only controls was recorded at 24 hours using a cell density meter designed for measurement of microbial growth (CO 8000 Biowave, VWR International, Pennsylvania, USA). To assess the effect of the studied compounds on microbial growth the absorbance of Female 2's microbiota cultured alone was compared to the absorbances of the microbiota incubated with trifluridine-only, tipiracil + trifluridine, clindamycin + trifluridine, and uridine + trifluridine (n = 3 for each compound) at the 24-hour timepoint. The microbiota-free control was used as the reference absorbance. Measurements were recorded inside the anaerobic chamber (A25 Sleeved Anaerobic Workstation, Don Whitley Scientific, Bingley, UK; containing 5 % CO_2, 5 % H_2, 90 % nitrogen).

2.2.8. Data analysis

Plots were constructed and statistical tests completed using GraphPad Prism (version 9.4.0, GraphPadInc, San Diego, US). Statistical significance was determined using one-way ANOVA tests with Tukey's multiple comparisons when comparing the means of samples for a single measurement. Two-way ANOVA tests with Tukey's multiple comparisons were employed to measure statistical significance between the means of samples for multiple measurements (such as the effects of independent interventions at different timepoints). The AUCs of the data corresponding to trifluorothymine formation, as measured by HPLC, were calculated using the dedicated tool in GraphPad. Error bars featured on plots represent standard deviation around the mean.

The kinetics of trifluridine degradation were explored by fitting the HPLC metabolism profiles to an exponential decay model in GraphPad Prism. A nonlinear regression model known as 'one phase decay', which corresponds to a first-order reaction, was utilised with a plateau constraint of 0.0. This constraint identified that total metabolism would result in 0.0 % of trifluridine remaining. The one phase decay model is suitable for determining the rate and half-life of drug metabolism as it assumes that the rate of drug metabolism is proportional to drug concentration. The curves were checked for goodness of fit by examining their R^2 values, this allowed the first-order assumptions to be accepted, *i.e.*, metabolising enzymes were not saturated during incubations. Trifluridine half-life was calculated via the GraphPad software using Eq. 1, which applies to first-order reactions.

$$t_{1/2} = \frac{ln2}{k}$$

Eq. 1. Calculation of substrate half-life for first-order reactions, where k is the degradation rate constant (Vertzoni et al., 2018).

3. Results and discussion

3.1. Microbial trifluridine metabolism is donor-specific

Fig. 4 shows the metabolism of trifluridine by the microbiota sourced

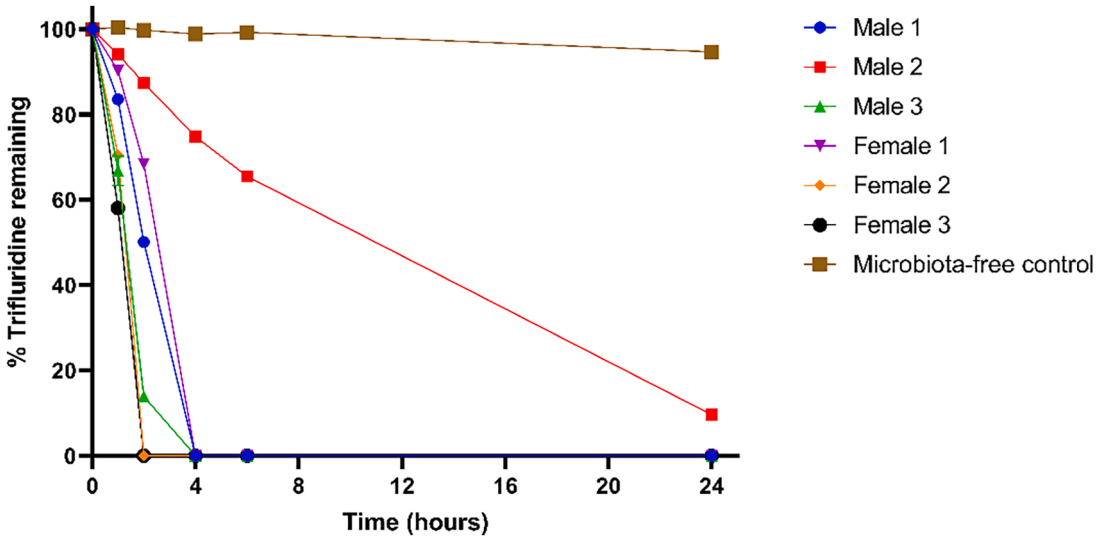

Fig. 4. Metabolism of trifluridine by the faecal microbiota sourced from six healthy human donors as measured by HPLC. N = 3 incubations were conducted per sample. Datapoints represent mean values with standard deviations.

from six human donors, as measured by HPLC. Clearly, there is inter-sample variability in the microbial drug transformation. Within the first two hours of incubation trifluridine transformation showed substantial variability: the microbiota cultured from Male 1 metabolised 49.9 ± 0.86 % of the drug; Male 2 metabolised 12.57 ± 0.35 %; Male 3 metabolised 86.10 ± 0.69 %; Female 1 metabolised 31.62 ± 1.24 %; and Female 2 and 3 metabolised all detectable trifluridine. These differences were statistically significant ($P < 0.0001$ between all donors, except for Females 2 and 3 which both showed 100 % metabolism).

By four hours, all donors' microbiota apart from Male 2 had completely metabolised the trifluridine, demonstrating that the microbiota from Male 2 were less efficient in inactivating the drug (Javdan et al., 2020). This finding was supported by the LC-MS results (shown in Section 3.2). Trifluridine metabolism followed first-order kinetics, showing that the rate of metabolism was proportional to the amount of drug remaining in the system and that enzyme saturation did not occur (Table 3) (Wolff, 2010). The microbial density of cultures after 24 hours' growth ranged from 6.80×10^8 - 1.12×10^9 CFU/mL, which is around two orders of magnitude below the bacterial density reported in the human colon (10^{10} - 10^{11} CFU/mL) (Martinez-Guryn et al., 2019). Therefore, the rate of trifluridine metabolism demonstrated in this study may be slower than that occurring within the colon.

Fig. 5 shows that the formation of trifluorothymine during the trifluridine incubations, as measured by HPLC. No trifluorothymine was detected in the microbiota-free control, evidencing that the microbiota was required for transformation of trifluridine to its inactive metabolite. The concentration of trifluorothymine produced by the microbiota was significantly different between all donors at the two-hour timepoint ($P < 0.0001$).

The microbiota samples from all donors aside from Male 2 produced increasing concentrations of trifluorothymine for the first 2 – 4 hours, reaching maximal trifluorothymine concentrations of 58.90 ± 8.79 μg/mL. After this peak, trifluorothymine concentration was observed to decrease. This decrease in trifluorothymine concentration could indicate either spontaneous degradation of the metabolite, or further transformation of the metabolite by the microbiota, a reaction that has not been described before. As the microbiota from Male 2 did not appear to significantly consume trifluorothymine it is reasonable to hypothesise that the microbiota was responsible for the observed decrease in trifluorothymine concentration; and that Male 2's microbiota had lower capacity to metabolite trifluorothymine than the other donors' samples.

Trifluridine half-life negatively correlated (R^2 = - 0.705) with the amount of trifluorothymine produced by each donor's microbiota, the latter being determined as the AUCs of the data presented in Fig. 5. This shows that a lower rate of trifluridine metabolism resulted in less formation of trifluorothymine, as to be expected during enzymatic conversion of one substrate to another. Again, these results highlight the variability of trifluridine metabolism by different individuals' microbiota. Prior research has shown that individuals from China and Fiji have significantly higher prevalence of the genes encoding thymidine and uridine phosphorylases in their faecal microbiomes compared to individuals from the USA, Spain, and Denmark (Javdan et al., 2020). The results of this study support that microbial metabolism of trifluridine is subject to inter-individual variability. However, it is pertinent to consider the current paucity of evidence linking *in vitro* drug-microbiome incubations with individual pharmacokinetic differences in *in vivo* (Jimonet et al., 2024). To establish an *in vitro-in vivo* relationship, it would be necessary to measure microbiome drug metabolism by different individuals' microbiota *in vitro* and then conduct pharmacokinetic analysis within the same individuals. This concept could first be investigated pre-clinically before investing in human studies. Nonetheless, there is some published work that links *in vitro* drug-microbiome incubations with *in vivo* findings (though not to study inter-individual variability). For example, a study by AstraZeneca has revealed that drug depletion by the faecal microbiota after 60 minutes could be predictive of permeability across the human colonic epithelium (Tannergren et al., 2014). Further, work by Kostantini et al. utilised the *in vitro* degradation kinetics of sulfinpyrazone to inform a physiologically based pharmacokinetic model (Kostantini et al., 2022). Variability in microbiome drug metabolism could provide the basis for differences

Table 3
The trifluridine half-lives during incubation with six human donors' microbiota (n = 3 incubations per donor sample). Half-lives were calculated based on first-order kinetics for the percentage of trifluridine remaining at all timepoints from 0 – 24 hours (resulting in 18 datapoints for fitting). The goodness of fit to first-order kinetics for each donor's microbial metabolism is presented as the R^2 value of the exponential decay model.

Microbiota donor	Trifluridine half-life (min)	Goodness of fit to first-order metabolism (R^2)
Male 1	91.74	0.9336
Male 2	504.96	0.9930
Male 3	59.40	0.9529
Female 1	106.26	0.8875
Female 2	53.33	0.8977
Female 3	47.01	0.9384

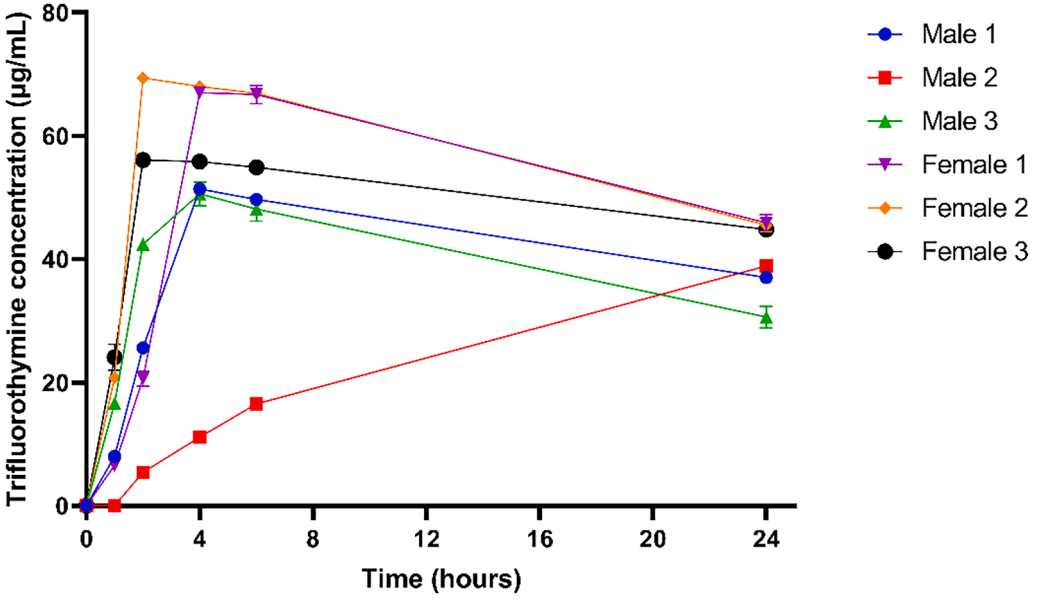

Fig. 5. Formation of trifluorothymine by the faecal microbiota sourced from six healthy human donors as measured by HPLC. N = 3 incubations were conducted per sample. Datapoints represent mean values with standard deviations.

in local/systemic drug bioavailability and efficacy between or within patients (McCoubrey et al., 2021; Vinarov et al., 2021).

3.2. *Trifluridine is transformed to multiple metabolites by the gut microbiota*

Based on the hypothesis that trifluorothymine was converted to subsequent metabolites by the donors' microbiota, LC-MS was utilised to further investigate the gut microbiome's trifluridine biotransformation. Fig. 6 presents an overview of five metabolites formed by the gut microbiota, four of these being linked to the microbiome for the first time. The reaction pathway leading to the metabolites' formation is presented in Fig. 3.

The five metabolites shown in Fig. 6 were sought in the samples

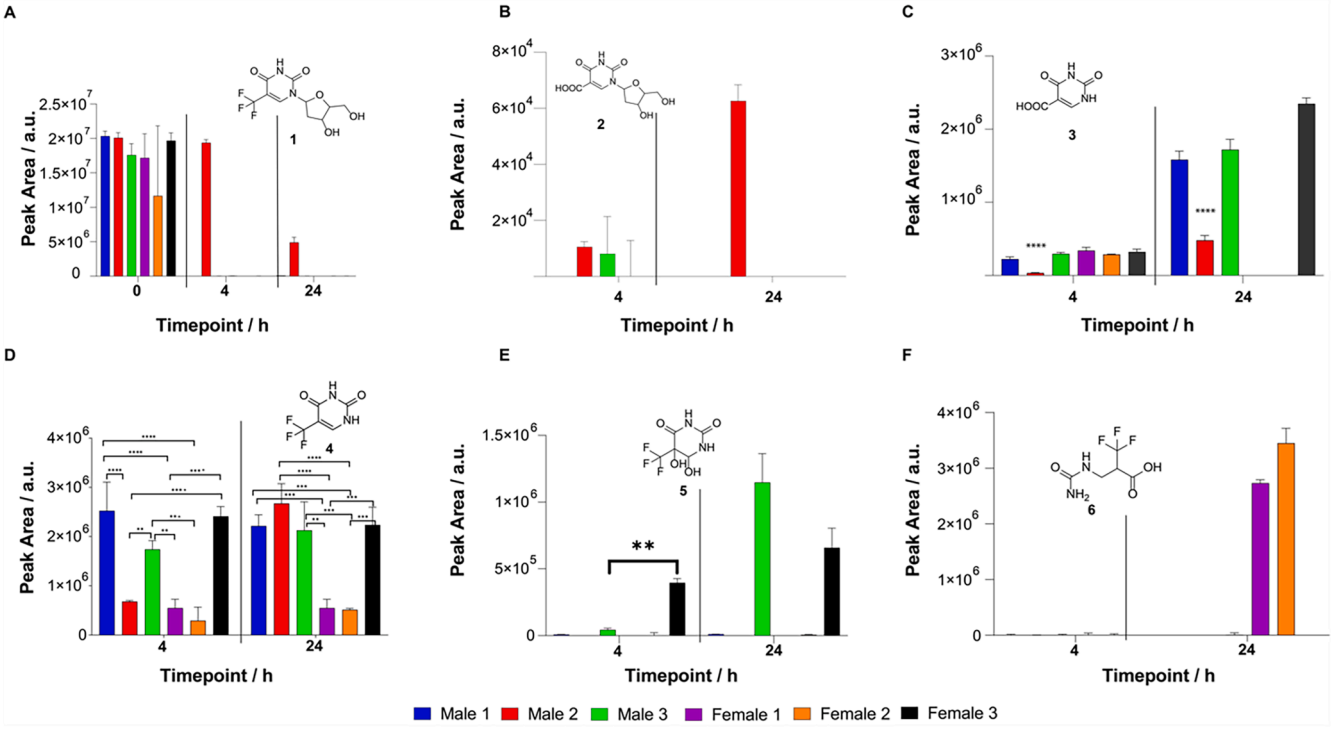

Fig. 6. Overview of trifluridine (A) and its five metabolites (B – F) as detected by ultra-high performance liquid chromatography coupled with high resolution tandem mass spectrometry in the faecal microbiota samples sourced from six healthy humans (n = 3 incubations per donor) at 4 and 24 hours. B: compound 2, 5-carboxy-2'-deoxy-uridine; C: compound 3, uracil-5-carboxylic acid; D: compound 4, trifluorothymine; E: compound 5, 5,6-dihydroxy-5-(trifluoromethyl)dihydropyrimidine-2,4(1H,3H)-dione; F: compound 6, 3,3,3-trifluoro-2-(ureidomethyl)propanoic acid. Vertical lines on plots separate results for the different timepoints. ** $P \leq 0.01$, *** $P \leq 0.001$, **** $P \leq 0.0001$.

based on their known formation during human and rat metabolism (Pavan-Langston and Nelson, 1979; Tandon et al., 1992; Voutsadakis, 2021). Compound 4, trifluorothymine (Figs. 5 and 6D), was also previously reported to be generated from trifluridine by gut bacteria in the study by Javdan et al. (Javdan et al., 2020). It is striking that compounds 2, 3, 5, and 6 can be formed by the gut microbiota as well as mammalian enzymes (Pavan-Langston and Nelson, 1979; Tandon et al., 1992; Voutsadakis, 2021). Additionally, Fig. 6 supports the inter-individual variability in microbial trifluridine metabolism that was noted in Section 3.1. Via the first biotransformation pathway (Fig. 3), the trifluoro group in trifluridine is converted into a carboxylic acid to obtain compound 2 and subsequently deglycosylated into compound 3. At 4 hours, compound 2 was only detected in 2/6 donors' samples, whereas compound 3 was present in all donors' samples (Figs. 6B and 6C). Notably, the amount of compound 3 in Male 2's samples at four hours was significantly reduced compared to the other donors ($P < 0.0001$). These findings suggest that Male 2's microbiota was less efficient in transforming compound 2 to compound 3. Moreover, as compound 2 was not detected in the samples from Male 1 and Females 1 – 3, the microbiota from these donors may have been highly efficient in converting trifluridine via this biotransformation pathway, leading to the intermediate compound 2 not being detected by four hours.

In trifluridine's second biotransformation pathway (Fig. 3) deglycosylation occurs to form compound 4 (trifluorothymine), which is subsequently metabolised via either: 1.) conversion of the trifluoro group to a carboxylic acid to form compound 3; 2.) hydroxylation of the alkene bond by multiple function oxidase to yield the cyclic diketone in compound 5; or, 3.) reduction of the alkene ring followed by a ring opening reaction to generate the carboxylic acid in compound 6. Trifluorothymine (Fig. 6D) was detected in all donors' samples and was variably transformed in a donor-specific manner. Compound 5 was detected in trace amounts in Male 1 and Female 2's samples and statistically higher amounts in Male 3 and Female 3's samples (Fig. 6E). In juxtaposition, compound 6 was detected in trace amounts in all donor samples at four hours and then in significantly elevated amounts in Female 1 and 2's samples after 24 hours (Fig. 6F). The HPLC analysis in Fig. 5 showed that all donor samples produced trifluorothymine, and that all but Male 2's microbiota appeared to consume trifluorothymine in an onward reaction. The LC-MS results correspond with the HPLC findings, whereby the onward biotransformation of trifluorothymine was characterised. In the case of Male 1 and 2's microbiota, no trifluorothymine metabolites were detected by LC-MS in significant amounts. This could signify that trifluorothymine was poorly converted by the microbiota (*e.g.*, in the case of Male 2), or that it was converted to other compounds that were not detected in this study.

These results illustrate the metabolic complexity of drug-microbiome interactions by showcasing the variable and multi-directional microbiome metabolism of trifluridine. During pharmaceutical development the identities and pharmacological profiles of drug metabolites should be characterised, though this is rarely undertaken in the case of microbiome drug metabolites. Where drugs are expected to reach the colon in significant concentrations then an assessment of their microbiome stability is particularly advisable (Jimonet et al., 2024). This is to identify if the microbiome is likely to produce metabolites with local and/or systemic pharmacological activity, that could affect the efficacy or toxicity profiles of investigatory drugs. The inter-donor variability noted for trifluridine's microbiome metabolism also demonstrates that drugs' biotransformation can be influenced by differences in microbiome composition and function. As such, the following sections of this study explore how microbiome drug metabolism is correlated with individual microbiome composition.

3.3. Individual metabolism of trifluridine is correlated with microbial composition

The ability to estimate individuals' rates of microbiome metabolism could afford multiple benefits, such as estimation of personalised pharmacokinetics. This was attempted for trifluridine in several ways. Firstly, metagenomics was utilised to better characterise the microbiota samples from each donor. This facilitated the use of simple linear regression to identify whether correlations existed between samples' features (presented in Table S2) and their rates of trifluridine metabolism.

3.3.1. Defining the taxonomic composition of the faecal microbiota samples

Fig. 7 shows the proportions of the most common bacterial genera and species in the faecal microbiota samples, as measured by metagenomic sequencing. All samples had different taxonomic compositions, potentially explaining their distinct trifluridine metabolism profiles. Inter-individual variability in faecal microbiome composition is widely accepted and well documented in the literature (Huttenhower et al., 2012; Qin et al., 2010; Tian et al., 2020; Yang et al., 2020; Zou et al., 2019).

At the phylum level, Firmicutes, Bacteroidetes, Actinobacteria and Proteobacteria (recently renamed as Bacillota, Bacteroidota, Actinomycetota, and Pseudomonadota), have been documented as the most common constituents of healthy individuals' faeces (Oren et al., 2021; Zou et al., 2019). The majority (11/13) of the genera shown in Fig. 7A belong to the Bacillota phylum (*e.g., Enterococcus, Lactobacillus, Clostridium,* and *Eubacterium*). The *Bacteroides* genus, which had high proportions in several samples, is a member of the Bacteroidota phylum. Therefore, the samples' phyla correspond with evidence that Bacillota and Bacteroidota are the most prevalent phyla in the faeces of healthy humans (Houtman et al., 2022; Stojanov et al., 2020).

Accordingly, 21/22 species shown in Fig. 7B are members of the Bacillota or Bacteroidota phyla. The notable exception is *Sutterella wadsworthensis*, a member of the Pseudomonadota phylum, which had sizeable representation in the samples sourced from Females 2 and 3. Though not a member of the Bacillota or Bacteroidota phyla, *Sutterella* species are reportedly abundant commensals of the GI tract (Hiippala et al., 2016). The compositions of the six samples are similar to those investigated by Javdan et al., who used the same growth medium as this study, and other studies reporting the composition of the faecal microbiome (Javdan et al., 2020; Martínez et al., 2013; Piancone et al., 2022). As such, the microbiota samples can be seen to reflect that expected in human faecal samples.

3.3.2. Linear regression identifies correlations for trifluridine's microbiome metabolism

Simple linear regression showed that the abundance of uridine and thymidine phosphorylase genes within the microbiota samples did not correlate with the percentage of trifluridine metabolised in the first two hours of incubation ($R^2 \leq 0.104$) or the trifluridine half-life ($R^2 \leq 0.182$), as measured by HPLC. It could be that the expression of these genes is more important than their abundance. Indeed, work by Heinken et al. recently revealed that microbial drug metabolism was better predicted by their AGORA2 model when they incorporated experimental metabolite uptake and secretion data into the model compared to only enzyme information extracted from genome annotation (Heinken et al., 2023). As such, it could be that information describing the expression of the enzymes could have better estimated the metabolism of trifluridine.

Similarly, the density of microbial cells in the stock microbiota samples did not correlate with two-hour trifluridine metabolism ($R^2 = 0.030$) or half-life ($R^2 = 0.007$). One reason for this could be that microbial density in the stock aliquots did not reflect their metabolic activity when cultured; *i.e.*, an aliquot with lower numbers of microbiota in the stock form could have high metabolic activity when cultured. This was potentially the case for the microbiota sourced from Male 1, which had the lowest microbial density in the stock aliquot but one of the highest after 24 hours' culture (Table S2).

Samples' microbial density at 24 h was weakly correlated with trifluridine metabolism at two hours ($R^2 = 0.374$) and half-life ($R^2 =$

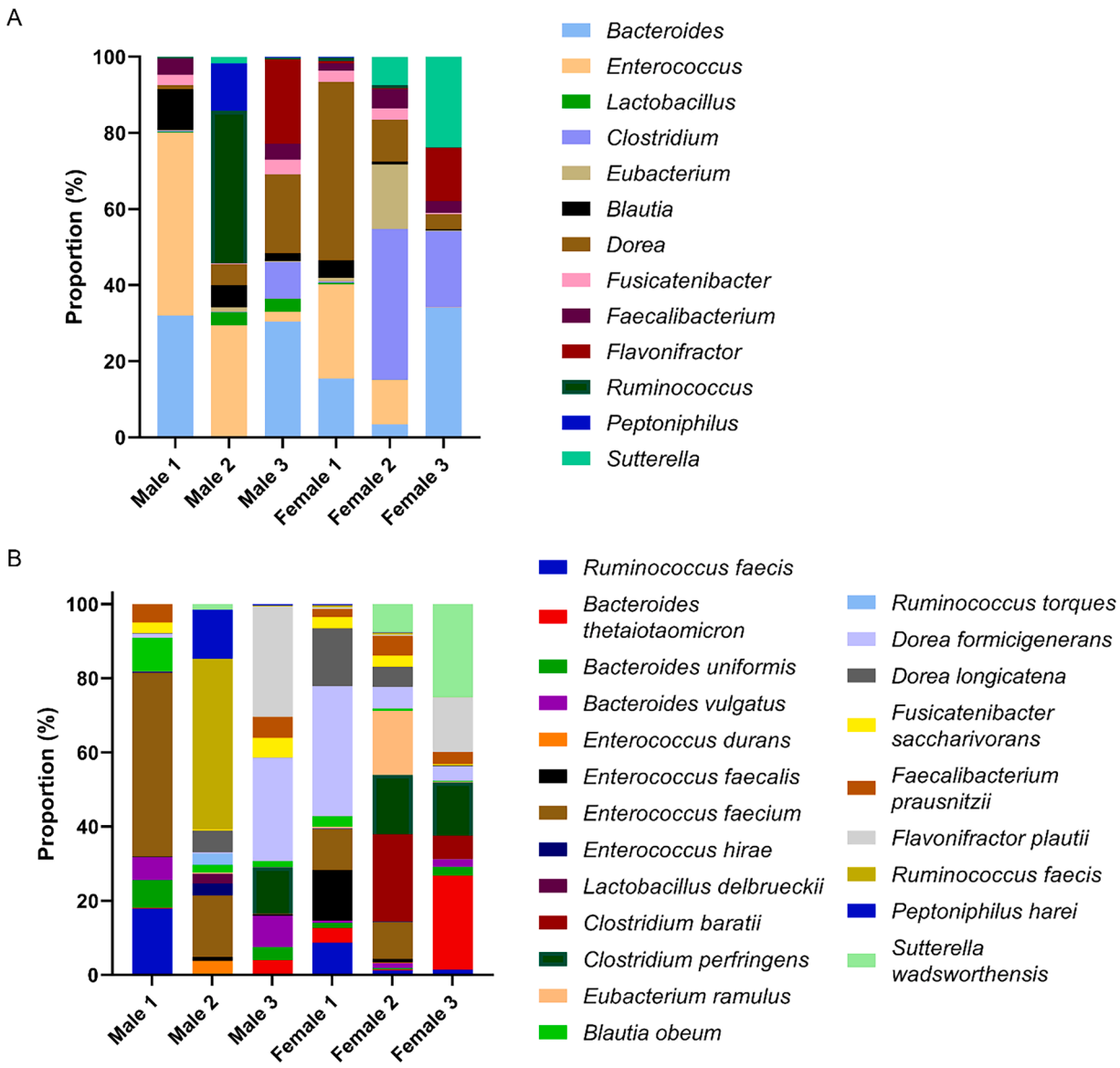

Fig. 7. The proportions of the most common genera (A, n = 13) and species (B, n = 22) in the faecal microbiota samples sourced from six healthy human donors. Samples were subject to metagenomic sequencing and taxonomic profiling using the MetaPhlAn tool that maps microbial marker genes to reference genomes (Truong et al., 2015).

0.260). It may be that the microbiota samples with the highest cell density after 24 hours also had higher metabolic activity at two hours due to greater cell division, and thus produced more drug-metabolising enzymes.

There were three bacterial taxa that correlated with the percentage of trifluridine metabolised in the first two hours of incubation: Clostridium ($R^2 = 0.6565$), Faecalibacterium ($R^2 = 0.6048$), and *Clostridium perfringens* ($R^2 = 0.8966$), By far, *Clostridium perfringens* had the strongest correlation (Fig. S4); its relative abundance was significantly higher in fast metabolisers of trifluridine (> 86 % metabolism after two hrs) compared to slow metabolisers (< 50 % metabolism after 2 hrs) ($P = 0.0047$). This is interesting as the functional profiling data obtained from metagenomic sequencing revealed that the microbiota from Male 3, Female 2, and Female 3 (the 'fast' metabolisers) contained *C. perfringens* that encoded for thymidine and uridine phosphorylase genes, whereas the other microbiota samples did not. Hence, the abundance of *C. perfringens* within the gut could be correlated with the rate at which individuals will metabolise trifluridine.

These results present important drug-microbiota relationships that have not been reported before. The associations between trifluridine metabolism, microbiota composition, and corresponding thymidine/uridine phosphorylase gene abundance could be further explored at a larger scale, to analyse if these features could become predictive markers of drug inactivation in patients.

For highly permeable drugs, Vertzoni et al. have estimated that drugs with a half-life of ≤ 95 min in the presence of the faecal microbiota will experience a clinically important reduction in bioavailability (Vertzoni et al., 2018). Regulatory bodies have classified trifluridine as having low intestinal permeability, and have labelled it as a Biopharmaceutics Classification System (BCS) class III compound (Center for Drug Evaluation and Research, 2015; European Medicines Agency, 2016). However, there is evidence that *in vivo* trifluridine absorption in the small intestine is higher than that measured with standard Caco-2 cells. When using human small intestinal epithelial cells trifluridine has a higher *in vitro* permeability, likely as these cells express concentrative nucleoside transporters (CNTs), which are thought to significantly contribute to trifluridine uptake (Takahashi et al., 2015). That said, CNTs are not expressed in the colon, hence trifluridine will likely have slow

absorption over the colonic epithelium, meaning that it will be exposed to the microbiota for longer than highly permeable drugs (Yvonne et al., 2007). In this regard, half-lives of > 95 min for poorly permeable drugs could still lead to clinically important reductions in bioavailability. The trifluridine half-lives during incubation with different donors' microbiota ranged from 47 – 505 min (Table 3). Therefore, it is possible that microbial metabolism would affect trifluridine bioavailability variably across patient populations if the drug were formulated for site-specific colon delivery. As such, various strategies to prevent the microbial metabolism of trifluridine were assessed.

3.3.3. *Microbial metabolism of trifluridine is preventable*

3.3.3.1. Clindamycin. Figs. 8A and 8B show the effect of clindamycin on trifluridine metabolism and trifluorothymine formation, as measured by HPLC. As expected, the antibiotic significantly reduced the rate of drug metabolism ($P < 0.0001$ from 1 - 6 h). The half-life of trifluridine in the presence of clindamycin (382.44 mins, goodness of fit to first-order metabolism (R^2): 0.9889) was substantially higher than without the antibiotic (53.33 mins). At two hours trifluridine was completely degraded in the presence of the microbiota, whereas the addition of clindamycin preserved 91.40 % (± 1.19) of the initial trifluridine concentration. As shown in Fig. 8B clindamycin significantly reduced the microbial production of trifluorothymine, which peaked at two hours in samples incubated without the antibiotic ($P < 0.0001$).

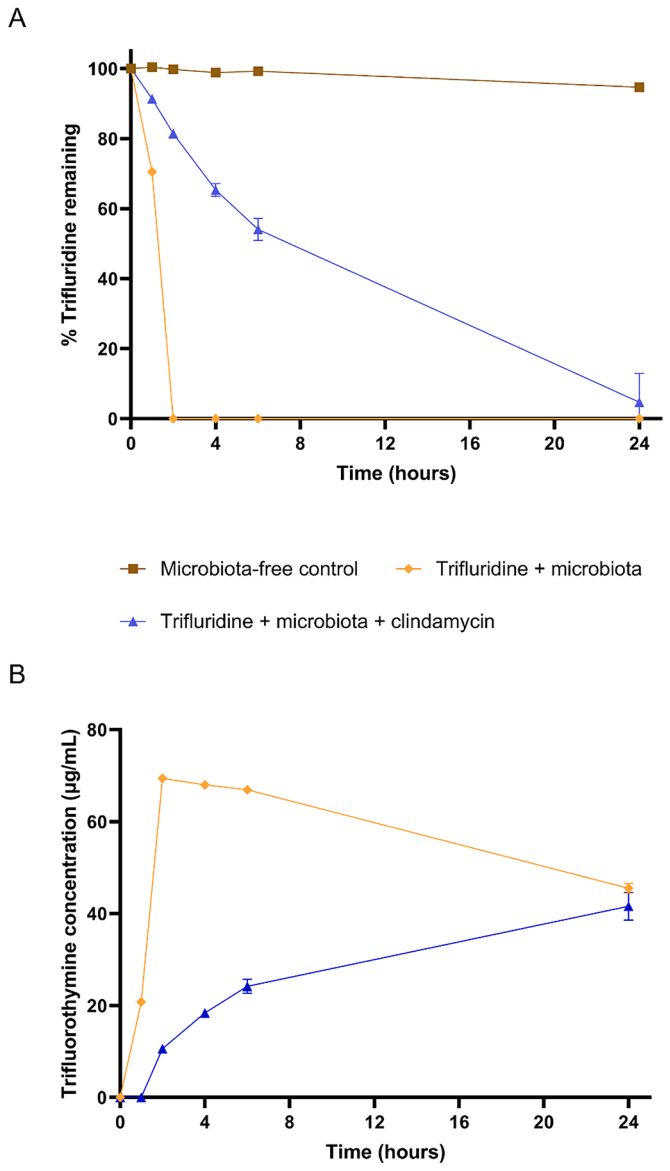

Fig. 8. Effect of clindamycin (1.0 mg/mL) on the metabolism of trifluridine (A) and formation of trifluorothymine (B) over 24 hours incubation with the microbiota sourced from Female Donor 2. N = 3 incubations were conducted per sample. Datapoints represent mean values with standard deviations.

Clindamycin is a lincosamide antibiotic and thus supresses protein synthesis by binding to bacterial RNA, resulting in primarily bacteriostatic and occasionally bactericidal effects (Pankey and Sabath, 2004). As such, clindamycin prevented bacterial synthesis of uridine and thymidine phosphorylases and thus reduced the rate of trifluridine metabolism. Functional profiling of the microbiota genes revealed the presence of the linA gene, which confers resistance to lincosamides, in several of the donor's microbiota samples (Brisson-Noël and Courvalin, 1986). However, linA was not detected in Donor 2's sample and hence antibiotic resistance was not expected to play a role in this experiment. Clindamycin is generally regarded to have excellent coverage of anaerobic gut bacteria (Levison Matthew et al., 1974).

Clindamycin was evidently effective in reducing trifluridine inactivation by the microbiota *in vitro*. As antibiotics are known to substantially alter the gut microbiome composition and functioning *in vivo*, it could thus be hypothesised that administration of broad-spectrum antibiotics, or antibiotics with selective action against inactivating the microbiota, could alter the half-life of microbiome-sensitive drugs within the human colon (Maier et al., 2021). That said, the administration of antibiotics for the indication of preserving colonic drug stability is clearly not appropriate, due to antimicrobial resistance and the negative and long-lasting consequences of antibiotic administration on the gut microbiome (Maier et al., 2021; McCoubrey et al., 2021; Mulder et al., 2020). These include increased risk of pathogen expansion, local inflammation, antimicrobial resistance, and even systemic diseases, such as metabolic disorders (Ramirez et al., 2020). Further, the gut microbiota play an important role in the human immune system, which is related to the effectiveness of some chemotherapeutics in colon cancer (Roberti et al., 2020). Therefore, these results do not present clindamycin as a strategy for enabling a colon-targeted trifluridine formulation for colorectal cancer, but seek to outline that an antibiotic significantly affected the biotransformation of trifluridine, and possibly by conjecture other drugs susceptible to microbiome metabolism (McCoubrey and Basit, 2022).

3.3.3.2. Tipiracil hydrochloride. Fig. 9A and B demonstrate the effect of tipiracil on the microbial metabolism of trifluridine and formation of trifluorothymine, respectively. Tipiracil significantly reduced trifluridine metabolism within the first two hours of incubation ($P < 0.0001$), however trifluridine was still completely inactivated after four hours. The formation of trifluorothymine was also delayed and significantly decreased in the presence of tipiracil ($P < 0.0001$ at all timepoints). These findings support that tipiracil inhibited the metabolic conversion of trifluridine, albeit not to the extent achieved by clindamycin (Fig. 8). Tipiracil's inhibitory effects were marginal at this concentration, which is relevant to its ratio with trifluridine in the Lonsurf® formulation. As such, higher concentrations of tipiracil would need to be screened to confirm that the compound could adequately prevent the microbiome's inactivation of trifluridine.

Tipiracil is formulated in the marketed product Lonsurf® at a molar ratio 1:0.5 as an inhibitor of human thymidine phosphorylase, an enzyme found in multiple human tissues (Kish and Uppal, 2016; Schwartz et al., 1995; Servier Laboratories Limited, 2020). These results reveal that tipiracil is likely also active against microbial variants of thymidine phosphorylase, which have different structures and substrate affinities compared to the human enzyme (Norman et al., 2004; Schinazi et al., 1992). As such, formulation of trifluridine with higher concentrations of tipiracil than that present in Lonsurf® could be an effective

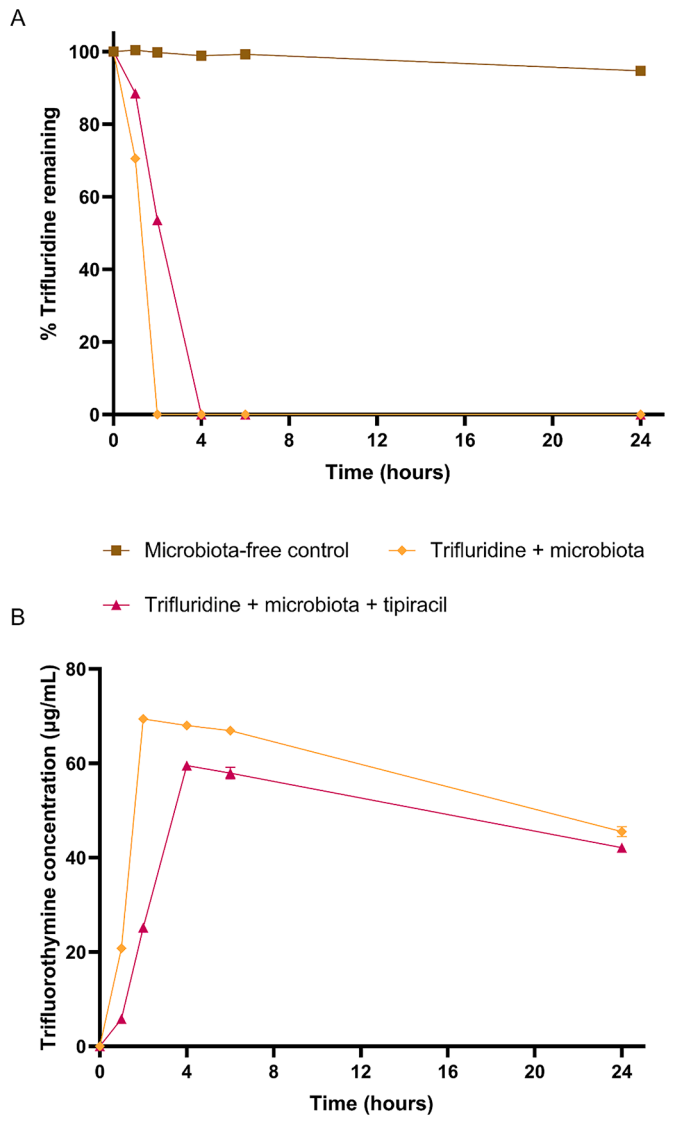

Fig. 9. The effect of tipiracil (81.83 µg/mL, to reflect the ratio of tipiracil to trifluridine found in the marketed formulation, Lonsurf®) on the metabolism of trifluridine (A) and formation of trifluorothymine (B) over 24 hours incubation with the microbiota sourced from Female Donor 2. N = 3 incubations were conducted per sample. Datapoints represent mean values with standard deviations.

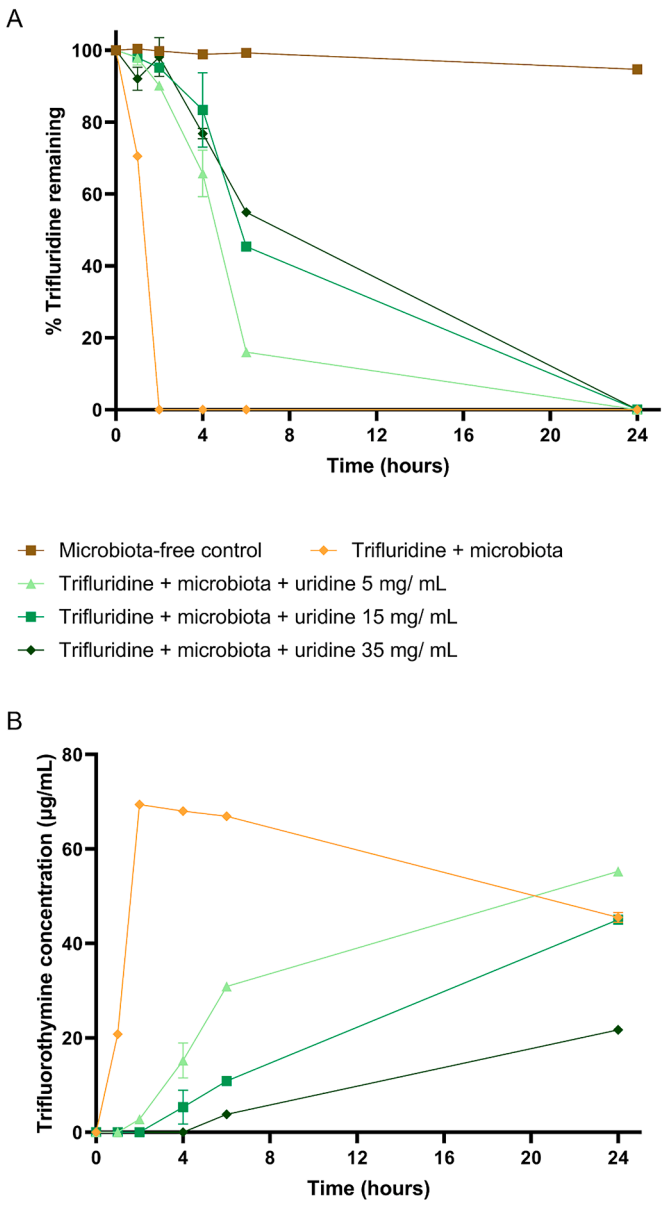

Fig. 10. The effect of ascending concentrations of uridine (5.0 - 35.0 mg/mL) on the metabolism of trifluridine (A) and formation of trifluorothymine (B) over 24 h incubation with the microbiota sourced from Female Donor 2. N = 3 incubations were conducted per sample. Datapoints represent mean values with standard deviations.

strategy for reducing trifluridine's microbiome-mediated inactivation.

That said, tipiracil is an expensive compound, therefore the high tipiracil concentration required to substantially spare microbial trifluridine inactivation in an oral dosage form would likely be economically inviable. Tipiracil has also recently been discovered to have antithrombotic actions; doses of 1.0 mg/kg tipiracil have significantly increased bleeding time in mice (Belcher et al., 2021). Hence, increasing tipiracil dose in a trifluridine product indicated for colorectal cancer could put patients at risk of bleeding-related adverse effects.

3.3.3.3. Uridine. Fig. 10A shows that all three concentrations of uridine prevented the metabolism of trifluridine when compared to trifluridine incubated alone with the microbiota ($P < 0.0001$ from 1 - 6 hours). For the first two hours, ≥ 90 % trifluridine remained intact in the presence of uridine, which was subsequently followed by first-order depletion. This initial plateau preceding metabolism was likely due to uridine's competitive inhibition of uridine phosphorylases; only when enough active sites were available for trifluridine did first-order metabolism take place. When incubated alone with the microbiota, trifluridine was completely metabolised after two hours, however addition of even 5.0 mg/mL uridine was sufficient to maintain 16.04 ± 0.47 % trifluridine at six hours. 15.0 mg/mL uridine increased trifluridine protection (45.37 ± 0.62 % trifluridine remaining at six hours) as did 35.0 mg/mL uridine (54.91 ± 0.70 % remaining at six hours).

At six hours, the extent that the different concentrations of uridine spared trifluridine metabolism was significantly different ($P \leq 0.0003$). The concentration of uridine *vs.* the percentage of remaining trifluridine at six hours was roughly linear ($R^2 = 0.7892$). The added trifluridine protection from 5.0 - 15.0 mg/mL uridine was larger than 15.0 - 35.0 mg/mL uridine, potentially showing that > 50 % uridine phosphorylase enzymes were competitively inhibited at 15.0 mg/mL. Within the first 4 hours of incubation the 15.0 and 35.0 mg/mL uridine concentrations protected trifluridine to a significantly greater extent than 1.0 mg/mL clindamycin ($P \leq 0.0009$). By six hours, the protective effects of 35.0

mg/mL uridine and clindamycin were statistically similar. Uridine's greater efficacy in the first four hours likely arose due to it fully saturating uridine phosphorylase in the starting system, whereas clindamycin prevented production of new inactivating enzymes but did not reduce the concentration of those already in the system. Hence, uridine provided immediate trifluridine protection whilst clindamycin did not.

Corresponding to trifluridine protection, the formation of trifluorothymine was reduced by the uridine interventions (Fig. 10B). The AUC of the trifluorothymine production when trifluridine was incubated alone with the microbiota was 1339.0 (μg/mL)*hours, with uridine this decreased to 840.7 (5.0 mg/mL uridine), 524.8 (15.0 mg/mL uridine), and 233.3 (μg/mL)*hours (35.0 mg/mL uridine). Uridine also prevented the decrease in trifluorothymine concentration between 2 - 24 hours, likely by delaying the metabolism of trifluridine and thus delaying trifluorothymine conversion.

These results demonstrate that competitive inhibition of microbial uridine phosphorylases was effective in delaying trifluridine metabolism by the microbiota. Uridine has a similar chemical structure to trifluridine, hence it successfully acted as a molecular decoy for microbiome drug metabolism. Over 75 % of the original trifluridine concentration was maintained by 35.0 mg/mL uridine at four hours, whereas without protection or with tipiracil the drug was completely metabolised. Mouse studies have demonstrated that higher trifluridine exposure is correlated with DNA incorporation in tumour cells and anti-tumour efficacy (Yamashita et al., 2015). As trifluridine has likely poor permeability across colonocytes, the longer its active form is retained the higher the probability it will permeate tumour cells intact (European Medicines Agency, 2016). Uridine is a substrate for small intestinal CNTs, thus would likely reduce trifluridine absorption in the small intestine. However, the colonic epithelium does not express CNTs hence trifluridine permeability should not be affected by uridine (Takahashi et al., 2015).

Uridine triacetate, a prodrug form of uridine, is licensed by the FDA for management of 5-FU toxicity (Jacob et al., 2022; Santos et al., 2017). For this indication, uridine triacetate is transformed to uridine *in vivo* by deacetylases and subsequently competes with fluorouridine triphosphate (a 5-FU metabolite) for incorporation into cellular RNA, leading to reduction of toxicity in healthy tissues. In clinical trials maximal plasma uridine concentrations were measured from 2 - 3 hours, suggesting that uridine is not absorbed so quickly across the GI epithelium that any trifluridine-protecting effects would be diminished *in vivo* (Ison et al., 2016). Uridine triacetate is a safe drug with low risk of adverse effects; only 2/135 patients discontinued treatment during clinical trials due vomiting, nausea, or diarrhoea (Ison et al., 2016). Trifluridine exerts its anti-tumour activity by reversibly inhibiting thymidylate synthase and competing with thymidine bases for incorporation into DNA (Burness and Duggan, 2016). As uridine is not involved in these pathways it is unlikely to interfere with trifluridine's mechanism of action. As such, uridine formulation with trifluridine represents a promising strategy for preventing microbiome metabolism of trifluridine in the colon. Similar enzyme saturation strategies could be trialled to prevent the microbiome metabolism of other drugs.

3.3.4. *Uridine promotes the growth of the gut microbiota*

Fig. 11 shows the effect of the five interventions on the growth of the intestinal microbiota over 24 hours. The effect of trifluridine alone is also presented. Trifluridine seems to be well suited for colonic delivery as it was not found to inhibit the growth of the microbiota; this was also true for tipiracil. As expected, clindamycin significantly reduced the growth of the microbiota ($P < 0.0001$), reducing average OD at 24 h by 61.8 %. In comparison, the uridine interventions significantly increased microbial proliferation, with the observed prebiotic effect peaking at 15.0 mg/mL uridine ($P < 0.0001$). This is the first time that the prebiotic effects of uridine for the gut microbiota have been described. Whilst this finding requires dedicated analysis, it is likely that addition of uridine increases nucleotide synthesis by the microbiota, as seen in experiments with mammalian cells (Morrison et al., 2019). Future work could explore whether uridine's prebiotic effects favour the expansion of specific species of the microbiota, and whether these effects could have associated health benefits. As uridine does not prevent the growth of the microbiota, its formulation with trifluridine for colonic delivery appears promising.

4. Conclusions

In this study the metabolism of trifluridine by the human faecal microbiota was successfully characterised and prevented. Incubation of trifluridine with the faecal microbiota sourced from six healthy human donors demonstrated significant variability in both trifluridine depletion and metabolite formation between donors' samples. LC-MS revealed five metabolites generated by the microbiota, four of which have not previously been linked to the gut microbiome. Metagenomic sequencing of samples allowed analysis of their composition and functional profiling of their genes. Using linear regression, a positive correlation was found between samples' relative abundances of *C. perfringens* and their rate of trifluridine metabolism. Notably, higher proportions of *C. perfringens* within samples were linked to a faster rate of trifluridine inactivation, arising from this species' encoding of

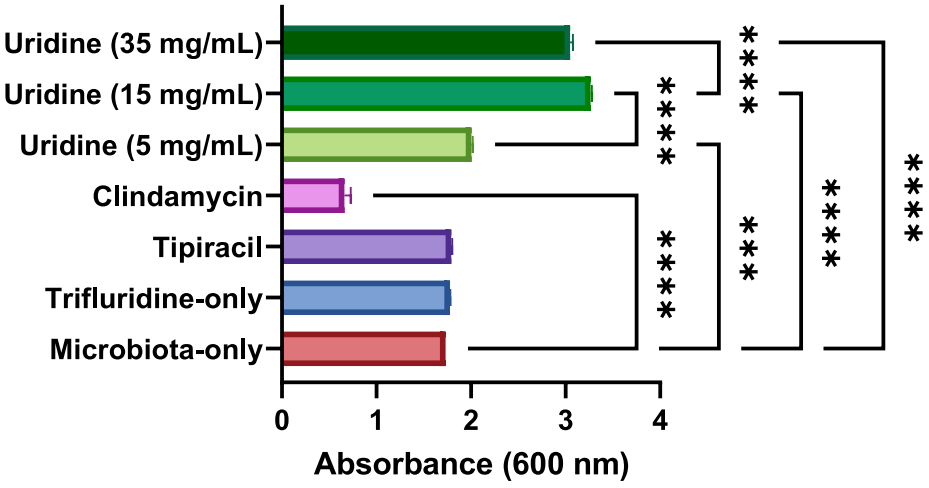

Fig. 11. The effect of trifluridine, trifluridine + tipiracil, trifluridine + clindamycin, and trifluridine with ascending concentrations of uridine, on the growth of the microbiota sourced from Female Donor 2. Absorbance represents the optical density of 24-hour microbial cultures at 600 nm. N = 3 incubations and measurements were conducted per intervention. *** $P \leq 0.001$, **** $P \leq 0.0001$.

thymidine and uridine phosphorylase genes. Having characterised the microbial metabolism of trifluridine, the focus was shifted to preventing its metabolism. The antibiotic clindamycin significantly reduced trifluridine inactivation, suggesting that antibiotics may have significant effects on drug-microbiome interactions *in vivo*. Tipiracil, which is formulated with trifluridine in the commercial Lonsurf® product, was also found to prevent drug inactivation to a lesser extent. Three concentrations of uridine successfully protected trifluridine metabolism via competitive inhibition of uridine phosphorylases. In the presence of 35.0 mg/mL uridine, 98.14 % trifluridine remained intact after two hours. Analysis of faecal microbial growth demonstrated that trifluridine and tipiracil had no effect on growth, clindamycin severely reduced growth, and uridine had previously unknown prebiotic effects. This worked aimed to highlight the importance of screening for drug-microbiome interactions, and to provide an example workflow wherein microbiome drug metabolism was investigated and preventative strategies were explored. Several valuable insights were afforded using simple *in vitro* techniques that could be cost-effectively applied in most drug development settings. The generated results provide a basis for *in vivo* validation of microbiome drug metabolism and provide lead strategies for enhancing drug stability in the colon.

CRediT authorship contribution statement

Laura E. McCoubrey: Writing – original draft, Visualization, Validation, Project administration, Methodology, Investigation, Formal analysis, Data curation, Conceptualization. **Chenghao Shen:** Validation, Methodology, Investigation, Formal analysis. **Sydney Mwasambu:** Writing – original draft, Validation, Software, Methodology, Investigation, Formal analysis, Data curation. **Alessia Favaron:** Writing – review & editing, Investigation, Formal analysis, Data curation. **Nannapat Sangfuang:** Writing – review & editing, Methodology, Investigation, Formal analysis, Data curation. **Stavrina Thomaidou:** Methodology, Investigation, Formal analysis, Data curation. **Mine Orlu:** Writing – review & editing, Supervision, Resources, Project administration. **Daniel Globisch:** Writing – review & editing, Validation, Supervision, Resources, Project administration, Funding acquisition. **Abdul W. Basit:** Writing – review & editing, Supervision, Project administration, Funding acquisition.

Declaration of competing interest

The authors declare that they have no known competing financial interests or personal relationships that could have appeared to influence the work reported in this paper. This work was conducted before Laura E. McCoubrey joined GSK and as such this work does not reflect the views of GSK.

Data availability

Data will be made available on request.

Acknowledgements

The valuable feedback from Dr David Shorthouse and Prof. Ben Forbes on this work was highly appreciated, as was the assistance from Intract Pharma Ltd. in processing the faecal microbiota samples. The authors acknowledge The Engineering and Physical Sciences Research Council [grant EP/S023054/1] to UCL School of Pharmacy for funding this work. Support was also obtained from the European Union's Horizon 2020 research and innovation programme under the Marie Skłodowska-Curie grant agreement No 956851. BioRender is also acknowledged for its use in designing Fig. 2 and the graphical abstract.

Supplementary materials

Supplementary material associated with this article can be found, in the online version, at doi:10.1016/j.ejps.2024.106922.

References

Allegretti, J.R., Fischer, M., Sagi, S.V., Bohm, M.E., Fadda, H.M., Ranmal, S.R., Budree, S., Basit, A.W., Glettig, D.L., de la Serna, E.L., Gentile, A., Gerardin, Y., Timberlake, S., Sadovsky, R., Smith, M., Kassam, Z., 2019. Fecal microbiota transplantation capsules with targeted colonic versus gastric delivery in recurrent clostridium difficile infection: a comparative cohort analysis of high and lose dose. Dig. Dis. Sci. 64, 1672–1678.

Ashburner, M., Ball, C.A., Blake, J.A., Botstein, D., Butler, H., Cherry, J.M., Davis, A.P., Dolinski, K., Dwight, S.S., Eppig, J.T., Harris, M.A., Hill, D.P., Issel-Tarver, L., Kasarskis, A., Lewis, S., Matese, J.C., Richardson, J.E., Ringwald, M., Rubin, G.M., Sherlock, G., 2000. Gene Ontology: tool for the unification of biology. Nat. Genet. 25, 25–29.

Awad, A., Madla, C.M., McCoubrey, L.E., Ferraro, F., Gavins, F.K.H., Buanz, A., Gaisford, S., Orlu, M., Siepmann, F., Siepmann, J., Basit, A.W., 2022. Clinical translation of advanced colonic drug delivery technologies. Adv. Drug Deliv. Rev. 181, 114076.

Beghini, F., McIver, L.J., Blanco-Míguez, A., Dubois, L., Asnicar, F., Maharjan, S., Mailyan, A., Manghi, P., Scholz, M., Thomas, A.M., Valles-Colomer, M., Weingart, G., Zhang, Y., Zolfo, M., Huttenhower, C., Franzosa, E.A., Segata, N., 2021. Integrating taxonomic, functional, and strain-level profiling of diverse microbial communities with bioBakery 3. Elife 10.

Belcher, A., Zulfiker, A.H.M., Li, O.Q., Yue, H., Gupta, A.S., Li, W., 2021. Targeting Thymidine Phosphorylase With Tipiracil Hydrochloride Attenuates Thrombosis Without Increasing Risk of Bleeding in Mice. Arterioscler. Thromb. Vasc. Biol. 41, 668–682.

Breitwieser, F.P., Baker, D.N., Salzberg, S.L., 2018. KrakenUniq: confident and fast metagenomics classification using unique k-mer counts. Genome Biol. 19, 198.

Brisson-Noël, A., Courvalin, P., 1986. Nucleotide sequence of gene linA encoding resistance to lincosamides in Staphylococcus haemolyticus. Gene 43, 247–253.

Buermans, H.P.J., den Dunnen, J.T., 2014. Next generation sequencing technology: Advances and applications. Biochimica et Biophysica Acta (BBA) - Molecular Basis of Disease 1842, 1932–1941.

Burness, C.B., Duggan, S.T., 2016. Trifluridine/Tipiracil: A Review in Metastatic Colorectal Cancer. Drugs 76, 1393–1402.

Center for Drug Evaluation and Research, 2015. Lonsurf tablets: clinical pharmacology amd biopharmaceutics review. U.S. Food and Drug Administration, FDA, Maryland, USA.

Chen, S., Zhou, Y., Chen, Y., Gu, J., 2018. fastp: an ultra-fast all-in-one FASTQ preprocessor. Bioinformatics. 34, i884–i890.

Eluru, A., Babu, S., 2020. A New Selective Separation method development and Validation of Trifluridine and Tipiracil and its degradents were characterized by LC-MS/MS/QTOF. J. Pharmaceut. Sci. Res. 12, 199–205.

European Medicines Agency, 2016. Assessment Report for Lonsurf, International non-proprietary name: trifluridine /tipiracil, in: (CHMP), C.f.M.P.f.H.U. (Ed.), London, UK.

Haiser, H.J., Gootenberg, D.B., Chatman, K., Sirasani, G., Balskus, E.P., Turnbaugh, P.J., 2013. Predicting and manipulating cardiac drug inactivation by the human gut bacterium Eggerthella lenta. Science 341, 295–298.

Heinken, A., Hertel, J., Acharya, G., Ravcheev, D.A., Nyga, M., Okpala, O.E., Hogan, M., Magnusdottir, S., Martinelli, F., Nap, B., Preciat, G., Edirisinghe, J.N., Henry, C.S., Fleming, R.M.T., Thiele, I., 2023. Genome-scale metabolic reconstruction of 7,302 human microorganisms for personalized medicine. Nat. Biotechnol.

Hiippala, K., Kainulainen, V., Kalliomaki, M., Arkkila, P., Satokari, R., 2016. Mucosal Prevalence and Interactions with the Epithelium Indicate Commensalism of Sutterella spp. Front. Microbiol. 7, 1706.

Houtman, T.A., Eckermann, H.A., Smidt, H., de Weerth, C., 2022. Gut microbiota and BMI throughout childhood: the role of firmicutes, bacteroidetes, and short-chain fatty acid producers. Sci. Rep. 12, 3140.

Huttenhower, C., Gevers, D., Knight, R., Abubucker, S., Badger, J.H., Chinwalla, A.T., Creasy, H.H., Earl, A.M., FitzGerald, M.G., Fulton, R.S., Giglio, M.G., Hallsworth-Pepin, K., Lobos, E.A., Madupu, R., Magrini, V., Martin, J.C., Mitreva, M., Muzny, D. M., Sodergren, E.J., Versalovic, J., Wollam, A.M., Worley, K.C., Wortman, J.R., Young, S.K., Zeng, Q., Aagaard, K.M., Abolude, O.O., Allen-Vercoe, E., Alm, E.J., Alvarado, L, Andersen, G.L., Anderson, S., Appelbaum, E., Arachchi, H.M., Armitage, G., Arze, C.A., Ayvaz, T., Baker, C.C., Begg, L., Belachew, T., Bhonagiri, V., Bihan, M., Blaser, M.J., Bloom, T., Bonazzi, V., Paul Brooks, J., Buck, G.A., Buhay, C. J., Busam, D.A., Campbell, J.L., Canon, S.R., Cantarel, B.L., Chain, P.S.G., Chen, I.M. A., Chen, L., Chhibba, S., Chu, K., Ciulla, D.M., Clemente, J.C., Clifton, S.W., Conlan, S., Crabtree, J., Cutting, M.A., Davidovics, N.J., Davis, C.C., DeSantis, T.Z., Deal, C., Delehaunty, K.D., Dewhirst, F.E., Deych, E., Ding, Y., Dooling, D.J., Dugan, S.P., Michael Dunne, W., Scott Durkin, A., Edgar, R.C., Erlich, R.L., Farmer, C.N., Farrell, R.M., Faust, K., Feldgarden, M., Felix, V.M., Fisher, S., Fodor, A.A., Forney, L.J., Foster, L., Di Francesco, V., Friedman, J., Friedrich, D.C., Fronick, C.C., Fulton, L.L., Gao, H., Garcia, N., Giannoukos, G., Giblin, C., Giovanni, M.Y., Goldberg, J.M., Goll, J., Gonzalez, A., Griggs, A., Gujja, S., Kinder Haake, S., Haas, B.J., Hamilton, H.A., Harris, E.L., Hepburn, T.A., Herter, B., Hoffmann, D.E., Holder, M.E., Howarth, C., Huang, K.H., Huse, S.M., Izard, J., Jansson, J.K., Jiang, H., Jordan, C., Joshi, V., Katancik, J.A., Keitel, W.A., Kelley, S.

T., Kells, C., King, N.B., Knights, D., Kong, H.H., Koren, O., Koren, S., Kota, K.C., Kovar, C.L., Kyrpides, N.C., La Rosa, P.S., Lee, S.L., Lemon, K.P., Lennon, N., Lewis, C.M., Lewis, L., Ley, R.E., Li, K., Liolios, K., Liu, B., Liu, Y., Lo, C.-C, Lozupone, C.A., Dwayne Lunsford, R., Madden, T., Mahurkar, A.A., Mannon, P.J., Mardis, E.R., Markowitz, V.M., Mavromatis, K., McCorrison, J.M., McDonald, D., McEwen, J., McGuire, A.L., McInnes, P., Mehta, T., Mihindukulasuriya, K.A., Miller, J.R., Minx, P.J., Newsham, I., Nusbaum, C., O'Laughlin, M., Orvis, J., Pagani, I., Palaniappan, K., Patel, S.M., Pearson, M., Peterson, J., Podar, M., Pohl, C., Pollard, K.S., Pop, M., Priest, M.E., Proctor, L.M., Qin, X., Raes, J., Ravel, J., Reid, J. G., Rho, M., Rhodes, R., Riehle, K.P., Rivera, M.C., Rodriguez-Mueller, B., Rogers, Y.-H, Ross, M.C., Russ, C., Sanka, R.K., Sankar, P., Fah Sathirapongsasuti, J., Schloss, J. A., Schloss, P.D., Schmidt, T.M., Scholz, M., Schriml, L., Schubert, A.M., Segata, N., Segre, J.A., Shannon, W.D., Sharp, R.R., Sharpton, T.J., Shenoy, N., Sheth, N.U., Simone, G.A., Singh, I., Smillie, C.S., Sobel, J.D., Sommer, D.D., Spicer, P, Sutton, G. G., Sykes, S.M., Tabbaa, D.G., Thiagarajan, M., Tomlinson, C.M., Torralba, M., Treangen, T.J., Truty, R.M., Vishnivetskaya, T.A., Walker, J., Wang, L., Wang, Z., Ward, D.V., Warren, W., Watson, M.A., Wellington, C., Wetterstrand, K.A., White, J. R., Wilczek-Boney, K., Wu, Y., Wylie, K.M., Wylie, T., Yandava, C., Ye, L., Ye, Y., Yooseph, S., Youmans, B.P., Zhang, L., Zhou, Y., Zhu, Y., Zoloth, L., Zucker, J.D., Birren, B.W., Gibbs, R.A., Highlander, S.K., Methé, B.A., Nelson, K.E., Petrosino, J.F., Weinstock, G.M., Wilson, R.K., White, O., 2012. The Human Microbiome project, C. Structure, function and diversity of the healthy human microbiome. Nature 486, 207–214.

Illumina, I., 2010. Technology Spotlight: Illumina® Sequencing, San Diego, USA.

International Council for Harmonisation of Technical Requirements for Pharmaceuticals for Human Use, 1995. ICH Q2(R2) Validation of analytical procedures. European Medicines Agency, London, UK.

Ison, G., Beaver, J.A., McGuinn Jr., W.D., Palmby, T.R., Dinin, J., Charlab, R., Marathe, A., Jin, R., Liu, Q., Chen, X.H., Ysern, X., Stephens, O., Bai, G., Wang, Y., Dorff, S.E., Cheng, J., Tang, S., Sridhara, R., Pierce, W., McKee, A.E., Ibrahim, A., Kim, G., Pazdur, R., 2016. FDA approval: uridine triacetate for the treatment of patients following fluorouracil or capecitabine overdose or exhibiting early-onset severe toxicities following administration of these drugs. Clin. Cancer Res. 22, 4545–4549.

Jacob, A., Sekkath Veedu, J., Selene, I., Raj, R., Kannan, L., Patel, R., 2022. Case report: Uridine triacetate in the management of delayed onset 5-fluorouracil toxicity: A case report and review of literature. Front. Pharmacol. 13, 977734.

Javdan, B., Lopez, J.G., Chankhamjon, P., Lee, Y.J., Hull, R., Wu, Q., Wang, X., Chatterjee, S., Donia, M.S., 2020. Personalized mapping of drug metabolism by the human gut microbiome. Cell 181, 1661–1679 e1622.

Jimonet, P., Druart, C., Blanquet-Diot, S., Boucinha, L., Kourula, S., Le Vacon, F., Maubant, S., Rabot, S., Van de Wiele, T., Schuren, F., Thomas, V., Walther, B., Zimmermann, M., 2024. Gut microbiome integration in drug discovery and development of small molecules. Drug Metab. Dispos.

Kang, C., Dhillon, S., Deeks, E.D., 2019. Trifluridine/Tipiracil: a review in metastatic gastric cancer. Drugs 79, 1583–1590.

Karatza, E., Vertzoni, M., Muenster, U., Reppas, C., 2016. The impact of handling and storage of human fecal material on bacterial activity. J. Pharm. Sci. 105, 3458–3461.

Kish, T., Uppal, P., 2016. Trifluridine/Tipiracil (Lonsurf) for the Treatment of Metastatic Colorectal Cancer. P. T. 41, 314–325.

Kostantini, C., Arora, S., Soderlind, E., Ceulemans, J., Reppas, C., Vertzoni, M., 2022. Usefulness of optimized human fecal material in simulating the bacterial degradation of sulindac and sulfinpyrazone in the lower intestine. Mol. Pharm. 19, 2542–2548.

Lee, J.R., Muthukumar, T., Dadhania, D., Taur, Y., Jenq, R.R., Toussaint, N.C., Ling, L., Pamer, E., Suthanthiran, M., 2015. Gut microbiota and tacrolimus dosing in kidney transplantation. PLoS. One 10, e0122399.

Levison Matthew, E., Bran Jose, L., Ries, K., 1974. Treatment of anaerobic bacterial infections with clindamycin-2-phosphate. Antimicrob. Agents Chemother 5, 276–280.

Maier, L., Goemans, C.V., Wirbel, J., Kuhn, M., Eberl, C., Pruteanu, M., Muller, P., Garcia-Santamarina, S., Cacace, E., Zhang, B., Gekeler, C., Banerjee, T., Anderson, E. E., Milanese, A., Lober, U., Forslund, S.K., Patil, K.R., Zimmermann, M., Stecher, B., Zeller, G., Bork, P., Typas, A., 2021. Unravelling the collateral damage of antibiotics on gut bacteria. Nature 599, 120–124.

Martinez-Guryn, K., Leone, V., Chang, E.B., 2019. Regional diversity of the gastrointestinal microbiome. Cell Host. Microbe 26, 314–324.

Martínez, I., Muller, C.E., Walter, J., 2013. Long-term temporal analysis of the human fecal microbiota revealed a stable core of dominant bacterial species. PLoS. One 8, e69621.

McConnell, E.L., Fadda, H.M., Basit, A.W., 2008. Gut instincts: explorations in intestinal physiology and drug delivery. Int. J. Pharm. 364, 213–226.

McCoubrey, L.E., Basit, A.W., 2022. Addressing drug–microbiome interactions: the role of healthcare professionals. Pharm. J. 308, 7958.

McCoubrey, L.E., Gaisford, S., Orlu, M., Basit, A.W., 2021. Predicting drug-microbiome interactions with machine learning. Biotechnol. Adv. 54, 107797.

Mehta, R.S., Mayers, J.R., Zhang, Y., Bhosle, A., Glasser, N.R., Nguyen, L.H., Ma, W., Bae, S., Branck, T., Song, K., Sebastian, L., Pacheco, J.A., Seo, H.S., Clish, C., Dhe-Paganon, S., Ananthakrishnan, A.N., Franzosa, E.A., Balskus, E.P., Chan, A.T., Huttenhower, C., 2023. Gut microbial metabolism of 5-ASA diminishes its clinical efficacy in inflammatory bowel disease. Nat. Med.

Morrison, C., Bandara, K., Wang, W., Zhang, L., Figueroa Jr., B., 2019. Improvement of growth rates through nucleoside media supplementation of CHO clones. Cytotechnology 71, 733–742.

Mulder, M., Radjabzadeh, D., Kiefte-de Jong, J.C., Uitterlinden, A.G., Kraaij, R., Stricker, B.H., Verbon, A., 2020. Long-term effects of antimicrobial drugs on the composition of the human gut microbiota. Gut. Microbes. 12, 1795492.

Norman, R.A., Barry, S.T., Bate, M., Breed, J., Colls, J.G., Ernill, R.J., Luke, R.W.A., Minshull, C.A., McAlister, M.S.B., McCall, E.J., McMiken, H.H.J., Paterson, D.S., Timms, D., Tucker, J.A., Pauptit, R.A., 2004. Crystal structure of human thymidine phosphorylase in complex with a small molecule inhibitor. Structure 12, 75–84.

Oksanen, Jari, Blanchet, F Guillaume, Kindt, Roeland, Legendre, Pierre, Minchin, Peter R, Ohara, RB, Simpson, Gavin L, Solymos, Peter, Henry H Stevens, M, Wagner, H., 2013. Package vegan. Commun. Ecol. Package. Version 29 ed.

Oren, A., Arahal, D.R., Rosselló-Móra, R., Sutcliffe, I.C., Moore, E.R.B., 2021. Emendation of rules 5b, 8, 15 and 22 of the international code of nomenclature of prokaryotes to include the rank of phylum. Int. J. Syst. Evol. Microbiol. 71.

Pankey, G.A., Sabath, L.D., 2004. Clinical relevance of bacteriostatic versus bactericidal mechanisms of action in the treatment of gram-positive bacterial infections. Clin. Infect. Dis. 38, 864–870.

Pavan-Langston, D., Nelson, D.J., 1979. Intraocular penetration of trifluridine. Am. J. Ophthalmol. 87, 814–818.

Peiris, M., Aktar, R., Reed, D., Cibert-Goton, V., Zdanaviciene, A., Halder, W., Robinow, A., Corke, S., Dogra, H., Knowles, C.H., Blackshaw, A., 2022. Decoy bypass for appetite suppression in obese adults: role of synergistic nutrient sensing receptors GPR84 and FFAR4 on colonic endocrine cells. Gut 71, 928–937.

Piancone, E., Fosso, B., Marzano, M., De Robertis, M., Notario, E., Oranger, A., Manzari, C., Bruno, S., Visci, G., Defazio, G., D'Erchia, A.M., Filomena, E., Maio, D., Minelli, M., Vergallo, I., Minelli, M., Pesole, G., 2022. Natural and after colon washing fecal samples: the two sides of the coin for investigating the human gut microbiome. Sci. Rep. 12, 17909.

Pritchard, S.E., Marciani, L., Garsed, K.C., Hoad, C.L., Thongborisute, W., Roberts, E., Gowland, P.A., Spiller, R.C., 2014. Fasting and postprandial volumes of the undisturbed colon: normal values and changes in diarrhea-predominant irritable bowel syndrome measured using serial MRI. Neurogastroenterol. Motil. 26, 124–130.

Qin, J., Li, R., Raes, J., Arumugam, M., Burgdorf, K.S., Manichanh, C., Nielsen, T., Pons, N., Levenez, F., Yamada, T., Mende, D.R., Li, J., Xu, J., Li, S., Li, D., Cao, J., Wang, B., Liang, H., Zheng, H., Xie, Y., Tap, J., Lepage, P., Bertalan, M., Batto, J.-M., Hansen, T., Le Paslier, D., Linneberg, A., Nielsen, H.B., Pelletier, E., Renault, P., Sicheritz-Ponten, T., Turner, K., Zhu, H., Yu, C., Li, S., Jian, M., Zhou, Y., Li, Y., Zhang, X., Li, S., Qin, N., Yang, H., Wang, J., Brunak, S., Doré, J., Guarner, F., Kristiansen, K., Pedersen, O., Parkhill, J., Weissenbach, J., Antolin, M., Artiguenave, F., Blottiere, H., Borruel, N., Bruls, T., Casellas, F., Chervaux, C., Cultrone, A., Delorme, C., Denariaz, G., Dervyn, R., Forte, M., Friss, C., van de Guchte, M., Guedon, E., Haimet, F., Jamet, A., Juste, C., Kaci, G., Kleerebezem, M., Knol, J., Kristensen, M., Layec, S., Le Roux, K., Leclerc, M., Maguin, E., Melo Minardi, R., Oozeer, R., Rescigno, M., Sanchez, N., Tims, S., Torrejon, T., Varela, E., de Vos, W., Winogradsky, Y., Zoetendal, E., Bork, P., Ehrlich, S.D., Wang, J., Meta, H. I.T.C., 2010. A human gut microbial gene catalogue established by metagenomic sequencing. Nature 464, 59–65.

Ramirez, J., Guarner, F., Bustos Fernandez, L., Maruy, A., Sdepanian, V.L., Cohen, H., 2020. Antibiotics as major disruptors of gut microbiota. Front. Cell Infect. Microbiol. 10, 572912.

Roberti, M.P., Yonekura, S., Duong, C.P.M., Picard, M., Ferrere, G., Tidjani Alou, M., Rauber, C., Iebba, V., Lehmann, C.H.K., Amon, L., Dudziak, D., Derosa, L., Routy, B., Flament, C., Richard, C., Daillère, R., Fluckiger, A., Van Seuningen, I., Chamaillard, M., Vincent, A., Kourula, S., Opolon, P., Ly, P., Pizzato, E., Becharef, S., Paillet, J., Klein, C., Marliot, F., Pietrantonio, F., Benoist, S., Scoazec, J.-Y., Dartigues, P., Hollebecque, A., Malka, D., Pagès, F., Galon, J., Gomperts Boneca, I., Lepage, P., Ryffel, B., Raoult, D., Eggermont, A., Vanden Berghe, T., Ghiringhelli, F., Vandenabeele, P., Kroemer, G., Zitvogel, L., 2020. Chemotherapy-induced ileal crypt apoptosis and the ileal microbiome shape immunosurveillance and prognosis of proximal colon cancer. Nat. Med. 26, 919–931.

Rowe, W.P.M., Winn, M.D., 2018. Indexed variation graphs for efficient and accurate resistome profiling. Bioinformatics. 34, 3601–3608.

Santos, C., Morgan, B.W., Geller, R.J., 2017. The successful treatment of 5-fluorouracil (5-FU) overdose in a patient with malignancy and HIV/AIDS with uridine triacetate. Am. J. Emerg. Med. 35, 802.e807-802.e808.

Schinazi, R.F., Peck, A., Sommadossi, J.-P., 1992. Substrate specificity of escherichia coli thymidine phosphorylase for pyrimidine nucleosides with anti-human immunodeficiency virus activity. Biochem. Pharmacol. 44, 199–204.

Schwartz, E.L., Baptiste, N., Wadler, S., Makower, D., 1995. Thymidine phosphorylase mediates the sensitivity of human colon carcinoma cells to 5-fluorouracil *. J. Biol. Chem. 270, 19073–19077.

Schymanski, E.L., Jeon, J., Gulde, R., Fenner, K., Ruff, M., Singer, H.P., Hollender, J., 2014. Identifying small molecules via high resolution mass spectrometry: communicating confidence. Environ. Sci. Technol. 48, 2097–2098.

Servier Laboratories Limited, 2020. Lonsurf 15 mg/6.14 mg film-coated Tablets. Electronic Medicines Compendium, Online.

Shaw, L.P., Bassam, H., Barnes, C.P., Walker, A.S., Klein, N., Balloux, F., 2019. Modelling microbiome recovery after antibiotics using a stability landscape framework. ISMe J. 13, 1845–1856.

Spanogiannopoulos, P., Kyaw, T.S., Guthrie, B.G.H., Bradley, P.H., Lee, J.V., Melamed, J., Malig, Y.N.A., Lam, K.N., Gempis, D., Sandy, M., Kidder, W., Van Blarigan, E.L., Atreya, C.E., Venook, A., Gerona, R.R., Goga, A., Pollard, K.S., Turnbaugh, P.J., 2022. Host and gut bacteria share metabolic pathways for anti-cancer drug metabolism. Nat. Microbiol.

Steinbakk, M., Lingaas, E., Carlstedt-Duke, B., Høverstad, T., Midtvedt, A.C., Norin, K.E., Midtvedt, T., 1992. Faecal concentration of ten antibiotics and influence on some microflora-associated characteristics (MACs). Microb. Ecol. Health Dis. 5, 269–276.
Stojanov, S., Berlec, A., Strukelj, B., 2020. The influence of probiotics on the firmicutes/bacteroidetes ratio in the treatment of obesity and inflammatory bowel disease. Microorganisms. 8.
the Suzek, B.E., Wang, Y., Huang, H., McGarvey, P.B., Wu, C.H., UniProt, C., 2015. UniRef clusters: a comprehensive and scalable alternative for improving sequence similarity searches. Bioinformatics. 31, 926–932.
Takahashi, K., Yoshisue, K., Chiba, M., Nakanishi, T., Tamai, I., 2015. Involvement of concentrative nucleoside transporter 1 in intestinal absorption of trifluridine using human small intestinal epithelial cells. J. Pharm. Sci. 104, 3146–3153.
Tandon, M., Kumar, P., Wiebe, G., Wiebe, L.I., 1992. Detection of new metabolites of trifluridine (F3TdR) using 19F NMR spectroscopy. Biochem. Pharmacol. 44, 2223–2228.
Tannergren, C., Borde, A., Borestrom, C., Abrahamsson, B., Lindahl, A., 2014. Evaluation of an *in vitro* faecal degradation method for early assessment of the impact of colonic degradation on colonic absorption in humans. Eur. J. Pharm. Sci. 57, 200–206.
Tao, X., Huang, W., Pan, L., Sheng, L., Qin, Y., Chen, L., Yu, L., Wu, G., Wan, J., Li, H., 2023. Optimizing ex vivo culture conditions to study human gut microbiome. ISMe Commun. 3.
Tian, J., Li, C., Dong, Z., Yang, Y., Xing, J., Yu, P., Xin, Y., Xu, F., Wang, L., Mu, Y., Guo, X., Sun, Q., Zhao, G., Gu, Y., Qin, G., Jiang, W., 2023. Inactivation of the antidiabetic drug acarbose by human intestinal microbial-mediated degradation. Nat. Metab.
Tian, L., Wang, X.W., Wu, A.K., Fan, Y., Friedman, J., Dahlin, A., Waldor, M.K., Weinstock, G.M., Weiss, S.T., Liu, Y.Y., 2020. Deciphering functional redundancy in the human microbiome. Nat. Commun. 11, 6217.
Truong, D.T., Franzosa, E.A., Tickle, T.L., Scholz, M., Weingart, G., Pasolli, E., Tett, A., Huttenhower, C., Segata, N., 2015. MetaPhlAn2 for enhanced metagenomic taxonomic profiling. Nat. Methods 12, 902–903.
Vallianatou, T., Lin, W., Bèchet, N.B., Correia, M.S., Shanbhag, N.C., Lundgaard, I., Globisch, D., 2021. Differential regulation of oxidative stress, microbiota-derived, and energy metabolites in the mouse brain during sleep. J. Cereb. Blood Flow Metab. 41, 3324–3338.
van Kessel, S.P., Frye, A.K., El-Gendy, A.O., Castejon, M., Keshavarzian, A., van Dijk, G., El Aidy, S., 2019. Gut bacterial tyrosine decarboxylases restrict levels of levodopa in the treatment of Parkinson's disease. Nat. Commun. 10, 310.
Varum, F., Cristina Freire, A., Bravo, R., Basit, A.W., 2020a. OPTICORE, an innovative and accurate colonic targeting technology. Int. J. Pharm. 583, 119372.
Varum, F., Cristina Freire, A., Fadda, H.M., Bravo, R., Basit, A.W., 2020b. A dual pH and microbiota-triggered coating (Phloral(TM)) for fail-safe colonic drug release. Int. J. Pharm. 583, 119379.
Verstockt, B., Alsoud, D., van Oostrom, J., Smith, J., Stylli, J., Singh, S., van Gennep, S., Rahimian, P., Sabino, J., Ferrante, M., Singh, S., D'Haens, G., Vermeire, S., 2022. Tofacitinib tissue exposure correlates with endoscopic outcome. J. Crohn's Colitis 16, i394–i395.
Vertzoni, M., Kersten, E., van der Mey, D., Muenster, U., Reppas, C., 2018. Evaluating the clinical importance of bacterial degradation of therapeutic agents in the lower intestine of adults using adult fecal material. Eur. J. Pharm. Sci. 125, 142–150.
Vinarov, Z., Abdallah, M., Agundez, J.A.G., Allegaert, K., Basit, A.W., Braeckmans, M., Ceulemans, J., Corsetti, M., Griffin, B.T., Grimm, M., Keszthelyi, D., Koziolek, M., Madla, C.M., Matthys, C., McCoubrey, L.E., Mitra, A., Reppas, C., Stappaerts, J., Steenackers, N., Trevaskis, N.L., Vanuytsel, T., Vertzoni, M., Weitschies, W., Wilson, C., Augustijns, P., 2021. Impact of gastrointestinal tract variability on oral drug absorption and pharmacokinetics: An UNGAP review. Eur. J. Pharmaceut. Sci. 162, 105812.
Voutsadakis, I.A., 2021. Biomarkers of Trifluridine-Tipiracil Efficacy. J. Clin. Med. 10.
Wolff, K., 2010. First-Order Elimination Kinetics. In: Stolerman, I.P. (Ed.), Encyclopedia of Psychopharmacology. Springer Berlin Heidelberg, Berlin, Heidelberg, p. 536. -536.
Wood, D.E., Salzberg, S.L., 2014. Kraken: ultrafast metagenomic sequence classification using exact alignments. Genome Biol. 15, R46.
Yadav, V., House, A., Matiz, S., McCoubrey, L.E., Bettano, K.A., Bhave, L., Wang, M., Fan, P., Zhou, S., Woodhouse, J.D., Poimenidou, E., Dou, L., Basit, A.W., Moy, L.Y., Saklatvala, R., Hegde, L.G., Yu, H., 2022. Ileocolonic-targeted JAK inhibitor: a safer and more effective treatment for inflammatory bowel disease. Pharmaceutics. 14.
Yadav, V., Mai, Y., McCoubrey, L.E., Wada, Y., Tomioka, M., Kawata, S., Charde, S., Basit, A.W., 2021. 5-Aminolevulinic acid as a novel therapeutic for inflammatory bowel disease. Biomedicines. 9.
Yamashita, F., Komoto, I., Oka, H., Kuwata, K., Takeuchi, M., Nakagawa, F., Yoshisue, K., Chiba, M., 2015. Exposure-dependent incorporation of trifluridine into DNA of tumors and white blood cells in tumor-bearing mouse. Cancer Chemother Pharmacol. 76, 325–333.
Yang, J., Pu, J., Lu, S., Bai, X., Wu, Y., Jin, D., Cheng, Y., Zhang, G., Zhu, W., Luo, X., Rossello-Mora, R., Xu, J., 2020. Species-Level Analysis of Human Gut Microbiota With Metataxonomics. Front. Microbiol. 11, 2029.
Yvonne, M., Jyrki, J.E., Jutta, D., Manfred, G.I., Christian, H., Michael, F., Gerd, A.K.-U., Stephan, R.V., 2007. Regional distribution of solute carrier mRNA expression along the human intestinal tract. Drug Metabol. Dispos. 35, 590.
Zimmermann, M., Zimmermann-Kogadeeva, M., Wegmann, R., Goodman, A.L., 2019. Mapping human microbiome drug metabolism by gut bacteria and their genes. Nature 570, 462–467.
Zou, Y., Xue, W., Luo, G., Deng, Z., Qin, P., Guo, R., Sun, H., Xia, Y., Liang, S., Dai, Y., Wan, D., Jiang, R., Su, L., Feng, Q., Jie, Z., Guo, T., Xia, Z., Liu, C., Yu, J., Lin, Y., Tang, S., Huo, G., Xu, X., Hou, Y., Liu, X., Wang, J., Yang, H., Kristiansen, K., Li, J., Jia, H., Xiao, L., 2019. 1,520 reference genomes from cultivated human gut bacteria enable functional microbiome analyses. Nat. Biotechnol. 37, 179–185.